Commun Nonlinear Sci Numer Simulat 18 (2013) 351–372

Contents lists available at SciVerse ScienceDirect

Commun Nonlinear Sci Numer Simulat

journal homepage: www.elsevier.com/locate/cnsns

Bifurcation analysis in a recurrent neural network model with delays

Yuting Ding [a,b], Weihua Jiang [a], Pei Yu [b,*]

[a] Department of Mathematics, Harbin Institute of Technology, Harbin 150001, China
[b] Department of Applied Mathematics, The University of Western Ontario, London, Ontario, Canada N6A 5B7

ARTICLE INFO

Article history:
Received 2 May 2012
Accepted 3 July 2012
Available online 15 July 2012

Keywords:
Recurrent neural network model
Hopf-zero bifurcation
Double Hopf bifurcation
Normal form
Multiple time scales

ABSTRACT

In this paper, we study the dynamical behaviors of a three-node recurrent neural network model with four discrete time delays. We study several types of bifurcation, and use the method of multiple time scales to derive the normal forms associated with Hopf-zero bifurcation, non-resonant and resonant double Hopf bifurcations. Moreover, bifurcations are classified in two-dimensional parameter space near these critical points, and numerical simulations are presented to demonstrate the applicability of the theoretical results.

1. Introduction

Recurrent neural networks (RNNs), containing cycles or feedback connections, have been used to learn dynamically varying input/output data and been successfully tackled in many practical applications (e.g., see [10,15,17,22,23]). Such applications heavily depend on the analysis of dynamical behaviors such as stability, periodic oscillation, bifurcation, or chaos [14,18,25]. As we all know, the signal transmission from one neuron to another is not instantaneous, and time delay may occur in the process of information storage in neural networks. Thus, time delay should be incorporated into the neural network models in order for the analysis to be more realistic. Therefore, much attention has been recently focused on the study of dynamics of neural network models with discrete or distributed delays (e.g., see [1,11,12,21,24,26,28,29,32]).

Ruiz et al. [23] proposed a fresh configuration of recurrent neural network model which finds its motivation in learning process and control systems. It is shown that a multi-node network is able to learn and replicate autonomously a particular class of time varying periodic signals. Furthermore, this network model was applied to control the repetitive motion of a two-link robot manipulator. Later on, Townley et al. [25] used monotone dynamical systems theory to discuss the existence of limit cycles in a three-node recurrent neural network, and to show that recurrent networks can learn and then replicate a permanent oscillation. As an important form of RNNs, Ruiz's neural network model has attracted much attention of researchers. For example, Gao and Zhang [9] displayed an effective technique to determine the number and the distribution of the equilibria of a three-node system, and further studied qualitative properties of the equilibria. Recently, Maleki et al. [18] investigated the dynamical behaviors of the Ruiz's model with three neurons in the vicinity of the Bogdanov–Takens bifurcation point. They observed complicated behaviors by varying the weights in the network when homoclinic and heteroclinic bifurcations emanate from the Bogdanov–Takens point. However, the effect of time delays on the Ruiz's network model was not considered in the literatures mentioned above. Further, Hajihosseini et al. [12] introduced the distributed time delays into the Ruiz's model, and studied the stability and Hopf bifurcation of this model with a strong kernel in the frequency

* Corresponding author. Fax: +1 519 661 3523.
E-mail addresses: yding66@uwo.ca (Y. Ding), jiangwh@hit.edu.cn (W. Jiang), pyu@uwo.ca (P. Yu).

1007-5704/$ - see front matter © 2012 Elsevier B.V. All rights reserved.
http://dx.doi.org/10.1016/j.cnsns.2012.07.002

domain. Feng et al. [6] discussed the existence of oscillations in a three-node recurrent neural network with two weight parameters and one time delay. Furthermore, Ensari and Arik [4,5] analyzed global stability of a neural network made up of more than three nodes with multiple delays. Feng et al. [7,8] investigated the existence of oscillations for a type of n-node recurrent neural network with time delays.

It is well known that delay differential equations (DDE) may exhibit higher codimension singularities more frequently than that in ordinary differential equations (ODE) [2,13]. To our best knowledge, many papers deal with high codimension bifurcations in DDE by using center manifold reduction (CMR) method (e.g., see [11,16,27]). With this method, one needs to first change the retarded equations to operator differential equations, and then decompose the solution space of their linearized form into stable and center manifolds. Then, with adjoint operator equations, one computes the center manifold by projecting the whole space to the center manifold, and finally calculates the normal form restricted to the center manifold. In particular, if we choose two discrete delays as two bifurcation parameters, we need to redefine inner product by using a new double integration for the CMR method. By comparison in computing normal forms of DDE, it has been found that the multiple time scales (MTS) method [19,30,31] is simpler than the CMR method. The multiple time scales method is systematic and can be directly applied to the original delayed nonlinear dynamical system, without application of center manifold theory [3,20]. Moreover, the MTS method, unlike the CMR method which involves integration, only involves algebraic manipulations, making it easier to implement in symbolic computation.

The purpose of this paper is to investigate the dynamical behaviors of Ruiz's recurrent neural network model, as shown in Fig. 1, which consists of three neurons connected by different nonlinear couplings with discrete time delays. We will use the MTS method to derive the normal forms for several types of high co-dimensional bifurcations in this model. In this network (see Fig. 1), $u(t) = y(t)$, where $u(t)$ is the input and $y(t)$ is the output. This neural network operates as follows: first, it receives a teaching signal $u(t)$ from the external environment. During that period, the network weights are self-adapted and $y(t)$ tracks $u(t)$. When the adaptation is completed, the system switches autonomously from the learning stage into a unity feedback configuration stage so that $y(t)$ replaces $u(t)$ and the periodic pattern is sustained.

The rest of the paper is organized as follows. First, we consider the existence of several types of bifurcation in Section 2. Then, in Sections 3 and 4, we use the MTS method to derive the normal forms associated with the Hopf-zero, non-resonant and resonant double Hopf critical points. Further, bifurcation analysis and numerical simulations are presented in Section 5, and finally, conclusion is drawn in Section 6.

2. Stability of the trivial equilibrium

The neural network with multiple time delays, shown in Fig. 1, can be described by a set of nonlinear differential equations as follows [6]:

$$\begin{aligned}
\dot{x_1}(t) &= -x_1(t) + f(x_2(t-\tau_2)),\\
\dot{x_2}(t) &= -x_2(t) + u(t),\\
\dot{x_3}(t) &= -x_3(t) + af(x_1(t-\tau_1)) + bf(x_2(t-\tau_3)),\\
y(t) &= f(x_3(t-\tau_4)),
\end{aligned} \tag{1}$$

where $x_i(t)$ $(i = 1, 2, 3)$ is the state of the ith neuron, a and b are the connection weights, $\tau_j's$ $(j = 1, 2, 3, 4)$ are non-negative time delays. Here, $u(t) = y(t)$, $u(t)$ is the input, and $y(t)$ the output. The triggering nonlinear function of the neurons takes the hyperbolic tangent function, i.e. $f(\cdot) = \tanh(\cdot)$.

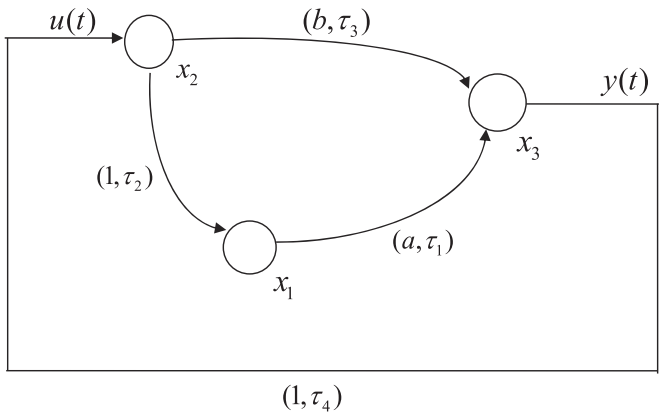

Fig. 1. Architecture of a network model consisting of three neurons with multiple time delays.

For simplicity, let $u_1(t) = x_1(t),\ u_2(t) = x_2(t-\tau_2)$ and $u_3(t) = x_3(t-\tau_2-\tau_4)$, then system (1) can be transformed into the following equations with two delays:

$$\begin{aligned} \dot{u}_1(t) &= -u_1(t) + f(u_2(t)),\\ \dot{u}_2(t) &= -u_2(t) + f(u_3(t)),\\ \dot{u}_3(t) &= -u_3(t) + af(u_1(t-\tau)) + bf(u_2(t-\sigma)), \end{aligned} \tag{2}$$

where $\tau = \tau_1 + \tau_2 + \tau_4$ and $\sigma = \tau_3 + \tau_4$.

The characteristic equation of (2), evaluated at the trivial equilibrium $(u_1, u_2, u_3) = (0,0,0)$, is given by

$$\lambda^3 + 3\lambda^2 + 3\lambda + 1 - (\lambda+1)be^{-\lambda\sigma} - ae^{-\lambda\tau} = 0. \tag{3}$$

There are several types of bifurcation.

Case 1 (*Fixed point bifurcation*). When $a + b = 1,\ \lambda = 0$ is a root of Eq. (3). If $a + b = 1$ and $b < 3$, then Eq. (3) with $\tau = \sigma = 0$ has a zero root and two roots with negative real part, and system (2) undergoes a fixed point bifurcation.

Case 2 (*Hopf bifurcation*). When $\sigma = 0$, Eq. (3) becomes

$$\lambda^3 + 3\lambda^2 + 3\lambda + 1 - (\lambda+1)b - ae^{-\lambda\tau} = 0. \tag{4}$$

If $a + b < 1$ and $8 + a - 2b > 0$, according to the Routh–Hurwitz criterion, all the roots of Eq. (4) have negative real part for $\tau = 0$.

To find possible periodic solutions, which may bifurcate from a Hopf critical point, let $\lambda = \mathrm{i}v(\mathrm{i}^2 = -1,\ v > 0)$ be a root of Eq. (4). Substituting $\lambda = \mathrm{i}v$ into (4) and separating the real and imaginary parts yields

$$\begin{aligned} -3v^2 + 1 - b &= a\cos(v\tau),\\ -v^3 + 3v - vb &= -a\sin(v\tau). \end{aligned} \tag{5}$$

Let $y = v^2$. Then it follows from (5) that

$$F(y) := y^3 + (3+2b)y^2 + (3+b^2)y + (b-1)^2 - a^2 = 0. \tag{6}$$

$F(y)$ has three roots, denoted by $y_k,\ k = 1,2,3$. If $y_k > 0$, then $v_k = \sqrt{y_k}$. Further, the time delay τ can be determined from (5) as

$$\tau_k^{(j)} = \begin{cases} \frac{1}{v_k}[\arccos(P_1) + 2j\pi], & Q_1 > 0,\\ \frac{1}{v_k}[2(j+1)\pi - \arccos(P_1)], & Q_1 < 0, \end{cases} \tag{7}$$

where $P_1 := \cos(v_k\tau_k^{(j)}) = \frac{-3v_k^2+1-b}{a}$, $Q_1 := \sin(v_k\tau_k^{(j)}) = \frac{v_k^3-3v_k+v_kb}{a}$, $k = 1,2,3;\ j = 0,1,2,\ldots$.

Let $\lambda(\tau) = \alpha(\tau) + \mathrm{i}v(\tau)$ be the root of (4) satisfying $\alpha(\tau_k^{(j)}) = 0,\ v(\tau_k^{(j)}) = v_k,\ k = 1,2,3;\ j = 0,1,2,\ldots$. Then, we have the transversality conditions:

$$\mathrm{Re}\left(\frac{\mathrm{d}\lambda}{\mathrm{d}\tau_k^{(j)}}\right)^{-1} = \frac{F'(v_k^2)}{a^2}, \tag{8}$$

where $k = 1,2,3;\ j = 0,1,2,\ldots$.

Lemma 2.1. *Suppose $a + b < 1$ and $8 + a - 2b > 0$. Then,*

(1) *if $\max_{k=1,2,3}\{y_k\} < 0$, where y_k is a root of (6), then all roots of Eq. (4) have negative real part for all $\tau \geqslant 0$;*
(2) *if there exists some $y_k > 0$, then there exists $\tau_0 = \min\{\tau_k^{(j)}\},\ k = 1,2,3;\ j = 0,1,2,\ldots$, such that all roots of Eq. (4) have negative real part for all $\tau \in [0,\tau_0)$, where $\tau_k^{(j)}$ $(k = 1,2,3;\ j = 0,1,2,\ldots)$ is given by (7).*

Further analysis is given for $\sigma > 0$. In this case, σ is regarded as a parameter for a fixed τ taken from the interval in which all roots of (4) have negative real part. Let $\lambda = \mathrm{i}\omega(\omega > 0)$ be a root of (3). Substituting $\lambda = \mathrm{i}\omega$ into (3) and separating the real and imaginary parts yields

$$\begin{aligned} &3\omega^2 - 1 + b\cos(\omega\sigma) + b\omega\sin(\omega\sigma) + a\cos(\omega\tau) = 0,\\ &\omega^3 - 3\omega + b\omega\cos(\omega\sigma) - b\sin(\omega\sigma) - a\sin(\omega\tau) = 0 \end{aligned}$$

from which we obtain

$$\begin{aligned} P_2 &:= \cos(\omega\sigma) = \frac{-\omega^4 + a\sin(\omega\tau)\omega + 1 - a\cos(\omega\tau)}{b(1+\omega^2)},\\ Q_2 &:= \sin(\omega\sigma) = -\frac{2\omega^3 + 2\omega + a\sin(\omega\tau) + \omega a\cos(\omega\tau)}{b(1+\omega^2)} \end{aligned} \tag{9}$$

and

$$E(\omega,\tau) := \omega^6 + 3\omega^4 - 2a\sin(\omega\tau)\omega^3 + [3 - b^2 + 6a\cos(\omega\tau)]\omega^2 + 6a\sin(\omega\tau)\omega - b^2 - 2a\cos(\omega\tau) + 1 + a^2 = 0, \quad (10)$$

where $\omega_k (k = 1,2,\ldots,k_0,\ k_0 \in \mathbb{N}^+)$ is a root of $E(\omega,\tau)$. If there exists some $\omega_k > 0$, then, we use (9) to obtain the time delay σ, given by

$$\sigma_k^{(j)} = \begin{cases} \frac{1}{\omega_k}[\arccos(P_2) + 2j\pi], & Q_2 \geqslant 0, \\ \frac{1}{\omega_k}[2(j+1)\pi - \arccos(P_2)], & Q_2 < 0, \end{cases} \quad (11)$$

where $k = 1,2,\ldots,k_0,\ j = 0,1,2,\ldots$.

Let $\lambda(\sigma) = \alpha(\sigma) + \mathrm{i}\omega(\sigma)$ be the root of (3) satisfying $\alpha(\sigma_k^{(j)}) = 0,\ \omega(\sigma_k^{(j)}) = \omega_k (k = 1,2,\ldots,k_0,\ j = 0,1,2,\ldots)$. Then the transversality conditions can be expressed as

$$\begin{aligned} \mathrm{Re}\left(\frac{\mathrm{d}\lambda}{\mathrm{d}\sigma_k^{(j)}}\right)^{-1} &= \frac{1}{b^2\omega(1+\omega^2)}[3\omega^5 + (6 - a\tau\cos(\omega\tau)\omega^3 - (3a\tau\sin(\omega\tau) + 3a\sin(\omega\tau))\omega^2 + (3 - b^2 \\ &\quad + 3a\tau\cos(\omega\tau) + 6a\cos(\omega\tau))\omega + a\tau\sin(\omega\tau) + 3a\sin(\omega\tau)], \end{aligned} \quad (12)$$

where $k = 1,2,\ldots,k_0,\ j = 0,1,2,\ldots$.

Theorem 2.2. *For some τ, if all roots of Eq. (4) have negative real part, then we have the following assertions.*

(1) *If Eq. (10) has no roots with positive real part, the trivial equilibrium of system (2) is asymptotically stable for all $\sigma \geqslant 0$.*
(2) *If Eq. (10) has at least one root $\omega_k > 0$ $(k = 1,2,\ldots,k_0)$ and $Re(\frac{\mathrm{d}\lambda}{\mathrm{d}\sigma_k^{(j)}}) \neq 0$, then there exists $\sigma_0 = \min\{\sigma_k^{(j)}\},\ k = 1,2,\ldots,k_0,\ j = 0,1,2,\ldots$, such that the trivial equilibrium of system (2) is asymptotically stable for $\sigma \in [0,\sigma_0)$, and system (2) undergoes a Hopf bifurcation from trivial equilibrium at $\sigma = \sigma_k^{(j)},\ k = 1,2,\ldots,k_0,\ j = 0,1,2,\ldots$, where $\sigma_k^{(j)}$ is given by (11).*

Case 3 (*Hopf-zero bifurcation*). Combining Cases 1 and 2, we have the following theorem.

Theorem 2.3. *Assume $a + b = 1$ and $b < 3$. For some τ, if all roots of Eq. (4) have negative real part, and Eq. (10) has at least one root $\omega_k > 0$ $(k = 1,2,\ldots,k_0)$ and $Re(\frac{\mathrm{d}\lambda}{\mathrm{d}\sigma_k^{(j)}}) \neq 0$ $(k = 1,2,\ldots,k_0,\ j = 0,1,2,\ldots)$, then system (2) undergoes a Hopf-zero bifurcation from the trivial equilibrium at $\sigma = \sigma_k^{(j)}$, where $\sigma_k^{(j)}$ is given by (11). In particular, when $\sigma = \min\{\sigma_k^{(j)}\}$ $(k = 1,2,\ldots,k_0,\ j = 0,1,2,\ldots)$, (3) has a zero root and a pair of purely imaginary roots, and all the other roots have negative real part.*

Case 4 (*Double Hopf bifurcation*). For some τ and σ, if Eq. (3) has two pairs of purely imaginary roots $\pm\mathrm{i}\omega_1$ and $\pm\mathrm{i}\omega_2$, and all the other roots have non-zero real part, then system (2) undergoes a double Hopf bifurcation. Assume $\omega_1 : \omega_2 = l_1 : l_2$. Then a double Hopf bifurcation with the ratio $l_1 : l_2$ appears. When $l_1,\ l_2 \in Z_+$, it is called an $l_1 : l_2$ resonant double Hopf bifurcation; otherwise, it is called a non-resonant double Hopf bifurcation.

3. Normal form of Hopf-zero bifurcation

In this section, by using the multiple time scales (MTS) method, we derive the normal form of system (2) associated with Hopf-zero bifurcation. We treat the connection weight a and the time delay σ as two bifurcation parameters. Suppose system (2) undergoes a Hopf-zero bifurcation from the trivial equilibrium at the critical point: $a = a_c,\ \sigma = \sigma_c$. The Taylor expansion of Eq. (2) truncated at the cubic order terms is as follows:

$$\dot{u}(t) = M_1u(t) + aM_2u(t-\tau) + bM_3u(t-\sigma) + f(u(t),u(t-\tau),u(t-\sigma)), \quad (13)$$

where

$$u(t) = \begin{pmatrix} u_1(t) \\ u_2(t) \\ u_3(t) \end{pmatrix}, \quad M_1 = \begin{pmatrix} -1 & 1 & 0 \\ 0 & -1 & 1 \\ 0 & 0 & -1 \end{pmatrix}, \quad M_2 = \begin{pmatrix} 0 & 0 & 0 \\ 0 & 0 & 0 \\ 1 & 0 & 0 \end{pmatrix}, \quad M_3 = \begin{pmatrix} 0 & 0 & 0 \\ 0 & 0 & 0 \\ 0 & 1 & 0 \end{pmatrix}$$

and

$$f(u(t),u(t-\tau),u(t-\sigma)) = \begin{pmatrix} -\frac{1}{3}u_2^3(t) \\ -\frac{1}{3}u_3^3(t) \\ -\frac{a}{3}u_1^3(t-\tau) - \frac{b}{3}u_2^3(t-\sigma) \end{pmatrix}.$$

Define linear equation

$$\dot{u}(t) = M_1u(t) + a_cM_2u(t-\tau) + bM_3u(t-\sigma_c)$$

as

$$\dot{u}(t) = L_c(u(t), u(t-\tau), u(t-\sigma_c)).$$

Suppose the characteristic equation of $\dot{u}(t) = L_c(u(t), u(t-\tau), u(t-\sigma_c))$ has a pair of purely imaginary roots $\pm i\omega$ and a zero root, and no other roots with zero real part. Let $h_1 = (h_{11}, h_{12}, h_{13})^{\mathrm{T}}$ and $h_2 = (h_{21}, h_{22}, h_{23})^{\mathrm{T}}$ be the two eigenvectors of the linear operator L_c corresponding to the eigenvalues $i\omega$ and 0, respectively. Further, let $h_1^* = (h_{11}^*, h_{12}^*, h_{13}^*)^{\mathrm{T}}$ and $h_2^* = (h_{21}^*, h_{22}^*, h_{23}^*)^{\mathrm{T}}$ be the two normalized eigenvectors of the adjoint operator L_c^* of the linear operator L_c corresponding to the eigenvalues $-i\omega$ and 0, respectively, satisfying the inner product

$$\langle h_i^*, h_i \rangle = \overline{h_i^{*\mathrm{T}}} h_i = 1, \quad i = 1, 2.$$

By a simple calculation, we have

$$\begin{aligned}
h_1 &= (h_{11}, h_{12}, h_{13})^{\mathrm{T}} = (1, 1+i\omega, (1+i\omega)^2)^{\mathrm{T}},\\
h_2 &= (h_{21}, h_{22}, h_{23})^{\mathrm{T}} = (1, 1, 1)^{\mathrm{T}},\\
h_1^* &= (h_{11}^*, h_{12}^*, h_{13}^*)^{\mathrm{T}} = \left(\frac{a e^{i\omega\tau}}{2(1-i\omega)^3 + a e^{i\omega\tau}}, \frac{(1-i\omega)^2}{2(1-i\omega)^3 + a e^{i\omega\tau}}, \frac{1-i\omega}{2(1-i\omega)^3 + a e^{i\omega\tau}}\right)^{\mathrm{T}},\\
h_2^* &= (h_{21}^*, h_{22}^*, h_{23}^*)^{\mathrm{T}} = \left(\frac{a}{a+2}, \frac{1}{a+2}, \frac{1}{a+2}\right)^{\mathrm{T}}.
\end{aligned} \tag{14}$$

Because the nonlinearity is cubic, we seek a uniform second-order approximate solution of system (13) in powers of $\epsilon^{1/2}$. Thus, the solution of (13) is assumed to take the form:

$$u(t) = \epsilon^{1/2} u^{(1)}(T_0, T_1, \cdots) + \epsilon^{3/2} u^{(2)}(T_0, T_1, \cdots) + \cdots, \tag{15}$$

where $u^{(j)} = (u_1^{(j)}, u_2^{(j)}, u_3^{(j)})^{\mathrm{T}}$, $j = 1, 2, \ldots$; $T_k = \epsilon^k t$, $k = 0, 1, \ldots$. The derivative with respect to t is now transformed into

$$\frac{\mathrm{d}}{\mathrm{d}t} = \frac{\partial}{\partial T_0} + \epsilon \frac{\partial}{\partial T_1} + \cdots = \mathrm{D}_0 + \epsilon \mathrm{D}_1 + \cdots,$$

where the differential operator $\mathrm{D}_i = \frac{\partial}{\partial T_i}$, $i = 0, 1, \ldots$.

We take perturbations as $a = a_c + \epsilon a_\epsilon$ and $\sigma = \sigma_c + \epsilon\sigma_\epsilon$ in (13). To deal with the delayed terms, we expand $u_i^{(j)}(T_0 - \sigma_c - \epsilon\sigma_\epsilon, T_1 - \epsilon(\sigma_c + \epsilon\sigma_\epsilon), \cdots)$ and $u_i^{(j)}(T_0 - \tau, T_1 - \epsilon\tau, \cdots)$ at $u_i^{(j)}(T_0 - \sigma_c, T_1)$ and $u_i^{(j)}(T_0 - \tau, T_1)$, respectively, where $i = 1, 2, 3$; $j = 1, 2, \ldots$. Then, substituting the solution (15) with the multiple scales into (13) and balancing the coefficients of $\epsilon^{n/2}$ $(n = 1, 3, 5, \ldots)$ yields a set of ordered linear differential equations.

First, for the $\epsilon^{1/2}$–order terms, we have

$$\mathrm{D}_0 u^{(1)} - M_1 u^{(1)} - a_c M_2 u_\tau^{(1)} - b M_3 u_{\sigma_c}^{(1)} = 0, \tag{16}$$

where

$$\begin{aligned}
u_\tau^{(1)} &= \left(u_1^{(1)}(T_0 - \tau, T_1), u_2^{(1)}(T_0 - \tau, T_1), u_3^{(1)}(T_0 - \tau, T_1)\right)^{\mathrm{T}},\\
u_{\sigma_c}^{(1)} &= \left(u_1^{(1)}(T_0 - \sigma_c, T_1), u_2^{(1)}(T_0 - \sigma_c, T_1), u_3^{(1)}(T_0 - \sigma_c, T_1)\right)^{\mathrm{T}}.
\end{aligned}$$

Since $\pm i\omega$ and 0 are the eigenvalues of the linear operator L_c, the solution of (16) can be expressed in the form of

$$u^{(1)}(T_0, T_1) = G_1(T_1) h_1 e^{i\omega T_0} + \overline{G}_1(T_1) \bar{h}_1 e^{-i\omega T_0} + G_2(T_1) h_2, \tag{17}$$

where h_j $(j = 1, 2)$ is given by (14).

Next, for the $\epsilon^{3/2}$–order terms of (13), we obtain

$$\mathrm{D}_0 u^{(2)} - M_1 u^{(2)} - a_c M_2 u_\tau^{(2)} - b M_3 u_{\sigma_c}^{(2)} = -\mathrm{D}_1 u^{(1)} - a_c \tau M_2 \mathrm{D}_1 u_\tau^{(1)} + a_\epsilon M_2 u_\tau^{(1)} - b\sigma_\epsilon M_3 \mathrm{D}_0 u_{\sigma_c}^{(1)} - b\sigma_c M_3 \mathrm{D}_1 u_{\sigma_c}^{(1)} + \tilde{f}_1, \tag{18}$$

where

$$\begin{aligned}
u_\tau^{(2)} &= \left(u_1^{(2)}(T_0 - \tau, T_1), u_2^{(2)}(T_0 - \tau, T_1), u_3^{(2)}(T_0 - \tau, T_1)\right)^{\mathrm{T}},\\
u_{\sigma_c}^{(2)} &= \left(u_1^{(2)}(T_0 - \sigma_c, T_1), u_2^{(2)}(T_0 - \sigma_c, T_1), u_3^{(2)}(T_0 - \sigma_c, T_1)\right)^{\mathrm{T}},\\
\tilde{f}_1 &= -\frac{1}{3}\left(\left(u_2^{(1)}(T_0, T_1)\right)^3, \left(u_3^{(1)}(T_0, T_1)\right)^3, a_c\left(u_1^{(1)}(T_0 - \tau, T_1)\right)^3 + b\left(u_2^{(1)}(T_0 - \sigma_c, T_1)\right)^3\right)^{\mathrm{T}}.
\end{aligned}$$

Substituting solution (17) into (18) and simplifying, we can obtain a linear nonhomogeneous equation for $u^{(2)}$:

$$\mathrm{D}_0 u^{(2)} - M_1 u^{(2)} - a_c M_2 u_\tau^{(2)} - b M_3 u_{\sigma_c}^{(2)} = m_1 e^{i\omega T_0} + \bar{m}_1 e^{-i\omega T_0} + m_2, \tag{19}$$

where $m_j = (m_j^{(1)}, m_j^{(2)}, m_j^{(3)})^{\mathrm{T}}$ $(j = 1, 2)$ with

$$m_1^{(1)} = -\frac{\partial G_1}{\partial T_1} - (1+\mathrm{i}\omega)^2(1-\mathrm{i}\omega)G_1^2\overline{G}_1 - (1+\mathrm{i}\omega)G_1G_2^2,$$

$$m_1^{(2)} = -(1+\mathrm{i}\omega)\frac{\partial G_1}{\partial T_1} - (1+\mathrm{i}\omega)^4(1-\mathrm{i}\omega)^2G_1^2\overline{G}_1 - (1+\mathrm{i}\omega)^2G_1G_2^2,$$

$$\begin{aligned} m_1^{(3)} = &-\frac{\partial G_1}{\partial T_1}(1+\mathrm{i}\omega)^2 - a_c\tau\frac{\partial G_1}{\partial T_1}\mathrm{e}^{-\mathrm{i}\omega\tau} + a_\epsilon G_1\mathrm{e}^{-\mathrm{i}\omega\tau} - b\sigma_\epsilon(1+\mathrm{i}\omega)\mathrm{i}\omega G_1\mathrm{e}^{-\mathrm{i}\omega\sigma_c} - b\sigma_c(1+\mathrm{i}\omega)\mathrm{e}^{-\mathrm{i}\omega\sigma_c}\frac{\partial G_1}{\partial T_1} - a_c\mathrm{e}^{-\mathrm{i}\omega\tau}G_1^2\overline{G}_1 \\ &- a_c\mathrm{e}^{-\mathrm{i}\omega\tau}G_1G_2^2 - b(1+\mathrm{i}\omega)^2(1-\mathrm{i}\omega)\mathrm{e}^{-\mathrm{i}\omega\sigma_c}G_1^2\overline{G}_1 - b(1+\mathrm{i}\omega)\mathrm{e}^{-\mathrm{i}\omega\sigma_c}G_1G_2^2, \end{aligned}$$

$$m_2^{(1)} = -\frac{\partial G_2}{\partial T_1} - 2(1+\mathrm{i}\omega)(1-\mathrm{i}\omega)G_1\overline{G}_1G_2 - \frac{1}{3}G_2^3,$$

$$m_2^{(2)} = -\frac{\partial G_2}{\partial T_1} - 2(1+\mathrm{i}\omega)^2(1-\mathrm{i}\omega)^2G_1\overline{G}_1G_2 - \frac{1}{3}G_2^3,$$

$$m_2^{(3)} = -\frac{\partial G_2}{\partial T_1} - a_c\tau\frac{\partial G_2}{\partial T_1} + a_\epsilon G_2 - b\sigma_c\frac{\partial G_2}{\partial T_1} - \frac{a_c}{3}G_2^3 - 2a_cG_1\overline{G}_1G_2 - 2b(1+\mathrm{i}\omega)(1-\mathrm{i}\omega)G_1\overline{G}_1G_2 - \frac{b}{3}G_2^3.$$

Nonhomogeneous equation (19) has a solution if and only if the so-called solvability condition is satisfied [19]. That is, the right-hand side of nonhomogeneous equation (19) is orthogonal to every solution of the adjoint homogeneous problem. Let $\langle h_1^*, m_1\rangle = 0$ and $\langle h_2^*, m_2\rangle = 0$, where h_j^* $(j = 1, 2)$ is given by (14). Then $\frac{\partial G_1}{\partial T_1}$ and $\frac{\partial G_2}{\partial T_1}$ are solved to yield

$$\begin{aligned} \frac{\partial G_1}{\partial T_1} &= \delta_1 G_1 + \delta_2 G_1^2\overline{G}_1 + \delta_3 G_1G_2^2, \\ \frac{\partial G_2}{\partial T_1} &= \alpha_2 G_2 + J_3G_2^3 + J_4G_1\overline{G}_1G_2, \end{aligned} \tag{20}$$

where

$$\begin{aligned} \delta_1 &= \frac{(1+\mathrm{i}\omega)\mathrm{e}^{-\mathrm{i}\omega\tau}a_\epsilon - \mathrm{i}(1+\mathrm{i}\omega)^2b\sigma_\epsilon\omega\mathrm{e}^{-\mathrm{i}\omega\sigma_c}}{2(1+\mathrm{i}\omega)^3 + a_c\mathrm{e}^{-\mathrm{i}\omega\tau} + a_c\tau\mathrm{e}^{-\mathrm{i}\omega\tau}(1+\mathrm{i}\omega) + b\sigma_c\mathrm{e}^{-\mathrm{i}\omega\sigma_c}(1+\mathrm{i}\omega)^2}, \\ \alpha_2 &= \frac{a_\epsilon}{a_c + 2 + a_c\tau + b\sigma_c}, \\ \delta_2 &= -\frac{(1+\mathrm{i}\omega)^5(1-\mathrm{i}\omega) + (1+\mathrm{i}\omega)^6(1-\mathrm{i}\omega)^2 + a_c\mathrm{e}^{-\mathrm{i}\omega\tau}(1+\mathrm{i}\omega)}{2(1+\mathrm{i}\omega)^3 + a_c\mathrm{e}^{-\mathrm{i}\omega\tau} + a_c\tau\mathrm{e}^{-\mathrm{i}\omega\tau}(1+\mathrm{i}\omega) + b\sigma_c\mathrm{e}^{-\mathrm{i}\omega\sigma_c}(1+\mathrm{i}\omega)^2}, \\ \delta_3 &= -\frac{2a_c(1+\mathrm{i}\omega)\mathrm{e}^{-\mathrm{i}\omega\tau} + (1+\mathrm{i}\omega)^4 + b(1+\mathrm{i}\omega)^2\mathrm{e}^{-\mathrm{i}\omega\sigma_c}}{2(1+\mathrm{i}\omega)^3 + a_c\mathrm{e}^{-\mathrm{i}\omega\tau} + a_c\tau\mathrm{e}^{-\mathrm{i}\omega\tau}(1+\mathrm{i}\omega) + b\sigma_c\mathrm{e}^{-\mathrm{i}\omega\sigma_c}(1+\mathrm{i}\omega)^2}, \\ J_3 &= -\frac{2a_c + 1 + b}{3(a_c + 2 + a_c\tau + b\sigma_c)}, \\ J_4 &= -\frac{2\left[a_c(1+\omega^2) + (1+\omega^2)^2 + a_c + b(1+\omega^2)\right]}{a_c + 2 + a_c\tau + b\sigma_c}. \end{aligned} \tag{21}$$

Eq. (20) is the normal form truncated at the cubic order terms, associated with the Hopf-zero bifurcation at the critical point: $a = a_c$ and $\sigma = \sigma_c$. Let $G_1 = r\mathrm{e}^{\mathrm{i}\theta}$ and $G_2 = z$. Substituting them into (20) yields the following normal form in cylindrical coordinates:

$$\begin{aligned} \frac{\mathrm{d}r}{\mathrm{d}t} &= \alpha_1 r + J_1r^3 + J_2rz^2, \\ \frac{\mathrm{d}z}{\mathrm{d}t} &= \alpha_2 z + J_3z^3 + J_4zr^2, \\ \frac{\mathrm{d}\theta}{\mathrm{d}t} &= \alpha_3 + J_5z^2 + J_6r^2, \end{aligned} \tag{22}$$

where $\alpha_1 = \mathrm{Re}(\delta_1)$, $\alpha_3 = \mathrm{Im}(\delta_1)$, $J_1 = \mathrm{Re}(\delta_2)$, $J_2 = \mathrm{Re}(\delta_3)$, $J_5 = \mathrm{Im}(\delta_2)$ and $J_6 = \mathrm{Im}(\delta_3)$, and δ_i $(i = 1, 2, 3)$, α_2 and J_i $(i = 3, 4)$ are given in (21).

4. Normal form of double Hopf bifurcation

In this section, we also use the MTS method to derive the normal form of double Hopf bifurcation in system (2). We treat the time delays σ and τ as two bifurcation parameters. Suppose system (2) undergoes a double Hopf bifurcation from the trivial equilibrium at the critical point: $\sigma = \sigma_c$, $\tau = \tau_c$. We will consider non-resonant and resonant cases, separately.

4.1. Non-resonant case

In this subsection, we consider non-resonant double Hopf bifurcation. Define linear equation

$$\dot{u}(t) = M_1 u(t) + aM_2 u(t-\tau_c) + bM_3 u(t-\sigma_c),$$

as

$$\dot{u}(t) = \widetilde{L}_c(u(t), u(t-\tau_c), u(t-\sigma_c)).$$

Suppose the characteristic equation of $\dot{u}(t) = \widetilde{L}_c(u(t), u(t-\tau_c), u(t-\sigma_c))$ has two pairs of purely imaginary roots $\pm i\omega_1$ and $\pm i\omega_2$, where $\omega_1 : \omega_2 = l_1 : l_2$ with l_1/l_2 irrational, and no other roots with zero real part. Let $g_1 = (g_{11}, g_{12}, g_{13})^{\mathrm{T}}$ and $g_2 = (g_{21}, g_{22}, g_{23})^{\mathrm{T}}$ be the two eigenvectors of the linear operator $\widetilde{L}_c$ corresponding to the eigenvalues $i\omega_1$ and $i\omega_2$, respectively. Further, let $g_1^* = (g_{11}^*, g_{12}^*, g_{13}^*)^{\mathrm{T}}$ and $g_2^* = (g_{21}^*, g_{22}^*, g_{23}^*)^{\mathrm{T}}$ be the two normalized eigenvectors of the adjoint operator $\widetilde{L}_c^*$ of linear operator $\widetilde{L}_c$ corresponding to the eigenvalues $-i\omega_1$ and $-i\omega_2$, respectively, satisfying the inner product

$$\langle g_i^*, g_i \rangle = \overline{g_i^*}^{\mathrm{T}} g_i = 1, \quad i = 1, 2.$$

With a simple calculation, we have

$$\begin{aligned} g_j &= (g_{j1}, g_{j2}, g_{j3})^{\mathrm{T}} = (1, 1 + i\omega_j, (1 + i\omega_j)^2)^{\mathrm{T}}, \\ g_j^* &= (g_{j1}^*, g_{j2}^*, g_{j3}^*)^{\mathrm{T}} = \left(\frac{a e^{i\omega_j \tau_c}}{2(1 - i\omega_j)^3 + a e^{i\omega_j \tau_c}}, \frac{(1 - i\omega_j)^2}{2(1 - i\omega_j)^3 + a e^{i\omega_j \tau_c}}, \frac{1 - i\omega_j}{2(1 - i\omega_j)^3 + a e^{i\omega_j \tau_c}} \right)^{\mathrm{T}}, \quad j = 1, 2. \end{aligned} \tag{23}$$

We choose perturbations as $\tau = \tau_c + \epsilon\tau_\epsilon$ and $\sigma = \sigma_c + \epsilon\sigma_\epsilon$ in (13). To deal with the delayed terms, we expand $u_i^{(j)}(T_0 - \tau_c - \epsilon\tau_\epsilon, T_1 - \epsilon(\tau_c + \epsilon\tau_\epsilon), \cdots)$ and $u_i^{(j)}(T_0 - \sigma_c - \epsilon\sigma_\epsilon, T_1 - \epsilon(\sigma_c + \epsilon\sigma_\epsilon), \cdots)$ at $u_i^{(j)}(T_0 - \tau_c, T_1)$ and $u_i^{(j)}(T_0 - \sigma_c, T_1)$, respectively, where $i = 1, 2, 3$; $j = 1, 2, \ldots$. Then, substituting the solution (15) with the multiple scales into (13) and balancing the coefficients of $\epsilon^{n/2}$ $(n = 1, 3, 5, \ldots)$ yields a set of ordered linear differential equations.

First, for the $\epsilon^{1/2}$–order terms, we have

$$\mathrm{D}_0 u^{(1)} - M_1 u^{(1)} - aM_2 u_{\tau_c}^{(1)} - bM_3 u_{\sigma_c}^{(1)} = 0, \tag{24}$$

where

$$\begin{aligned} u_{\tau_c}^{(1)} &= \left(u_1^{(1)}(T_0 - \tau_c, T_1), u_2^{(1)}(T_0 - \tau_c, T_1), u_3^{(1)}(T_0 - \tau_c, T_1) \right)^{\mathrm{T}}, \\ u_{\sigma_c}^{(1)} &= \left(u_1^{(1)}(T_0 - \sigma_c, T_1), u_2^{(1)}(T_0 - \sigma_c, T_1), u_3^{(1)}(T_0 - \sigma_c, T_1) \right)^{\mathrm{T}}. \end{aligned}$$

Since $\pm i\omega_1$ and $\pm i\omega_2$ are the eigenvalues of the linear operator $\widetilde{L}_c$, the solution of (24) can be expressed in the form of

$$u^{(1)}(T_0, T_1) = H_1(T_1) g_1 e^{i\omega_1 T_0} + \overline{H}_1(T_1) \bar{g}_1 e^{-i\omega_1 T_0} + H_2(T_1) g_2 e^{i\omega_2 T_0} + \overline{H}_2(T_1) \bar{g}_2 e^{-i\omega_2 T_0}, \tag{25}$$

where g_j $(j = 1, 2)$ is given by (23).

Next, for the $\epsilon^{3/2}$–order terms of (13), we obtain

$$\mathrm{D}_0 u^{(2)} - M_1 u^{(2)} - aM_2 u_{\tau_c}^{(2)} - bM_3 u_{\sigma_c}^{(2)} = -\mathrm{D}_1 u^{(1)} - a\tau_\epsilon M_2 \mathrm{D}_0 u_{\tau_c}^{(1)} - a\tau_c M_2 \mathrm{D}_1 u_{\tau_c}^{(1)} - b\sigma_\epsilon M_3 \mathrm{D}_0 u_{\sigma_c}^{(1)} - b\sigma_c M_3 \mathrm{D}_1 u_{\sigma_c}^{(1)} + \tilde{f}_2, \tag{26}$$

where

$$\begin{aligned} u_{\tau_c}^{(2)} &= \left(u_1^{(2)}(T_0 - \tau_c, T_1), u_2^{(2)}(T_0 - \tau_c, T_1), u_3^{(2)}(T_0 - \tau_c, T_1) \right)^{\mathrm{T}}, \\ u_{\sigma_c}^{(2)} &= \left(u_1^{(2)}(T_0 - \sigma_c, T_1), u_2^{(2)}(T_0 - \sigma_c, T_1), u_3^{(2)}(T_0 - \sigma_c, T_1) \right)^{\mathrm{T}}, \end{aligned}$$

$$\tilde{f}_2 = -\frac{1}{3} \left(\left(u_2^{(1)}(T_0, T_1) \right)^3, \left(u_3^{(1)}(T_0, T_1) \right)^3, a \left(u_1^{(1)}(T_0 - \tau_c, T_1) \right)^3 + b \left(u_2^{(1)}(T_0 - \sigma_c, T_1) \right)^3 \right)^{\mathrm{T}}.$$

Substituting solution (25) into (26) and simplifying, we obtain a linear nonhomogeneous equation for $u^{(2)}$:

$$\mathrm{D}_0u^{(2)} - M_1u^{(2)} - aM_2u^{(2)}_{\tau_c} - bM_3u^{(2)}_{\sigma_c} = n_1\mathrm{e}^{\mathrm{i}\omega_1T_0} + \bar{n}_1\mathrm{e}^{-\mathrm{i}\omega_1T_0} + n_2\mathrm{e}^{\mathrm{i}\omega_2T_0} + \bar{n}_2\mathrm{e}^{-\mathrm{i}\omega_2T_0}, \tag{27}$$

where $n_j = (n_j^{(1)}, n_j^{(2)}, n_j^{(3)})^{\mathrm{T}}$ $(j = 1, 2)$ with

$$n_j^{(1)} = -\frac{\partial H_j}{\partial T_1} - (1+\mathrm{i}\omega_j)^2(1-\mathrm{i}\omega_j)H_j^2\overline{H}_j - 2(1+\mathrm{i}\omega_j)(1+\mathrm{i}\omega_{3-j})(1-\mathrm{i}\omega_{3-j})H_jH_{3-j}\overline{H}_{3-j},$$

$$n_j^{(2)} = -(1+\mathrm{i}\omega_j)\frac{\partial H_j}{\partial T_1} - 2(1+\mathrm{i}\omega_j)^2(1+\mathrm{i}\omega_{3-j})^2(1-\mathrm{i}\omega_{3-j})^2H_jH_{3-j}\overline{H}_{3-j} - (1+\mathrm{i}\omega_j)^4(1-\mathrm{i}\omega_j)^2H_j^2\overline{H}_j,$$

$$\begin{aligned} n_j^{(3)} = &-\frac{\partial H_j}{\partial T_1}(1+\mathrm{i}\omega_j)^2 - \mathrm{i}\omega_j a\tau_\epsilon H_j\mathrm{e}^{-\mathrm{i}\omega_j\tau_c} - a\tau_c\frac{\partial H_j}{\partial T_1}\mathrm{e}^{-\mathrm{i}\omega_j\tau_c} - b\sigma_\epsilon(1+\mathrm{i}\omega_j)\mathrm{i}\omega_jH_j\mathrm{e}^{-\mathrm{i}\omega_j\sigma_c} \\ &- b\sigma_c(1+\mathrm{i}\omega_j)\mathrm{e}^{-\mathrm{i}\omega_j\sigma_c}\frac{\partial H_j}{\partial T_1} - 2a\mathrm{e}^{-\mathrm{i}\omega_j\tau_c}H_jH_{3-j}\overline{H}_{3-j} - a\mathrm{e}^{-\mathrm{i}\omega_j\tau_c}H_j^2\overline{H}_j \\ &- 2b(1+\mathrm{i}\omega_j)(1+\mathrm{i}\omega_{3-j})(1-\mathrm{i}\omega_{3-j})\mathrm{e}^{-\mathrm{i}\omega_j\sigma_c}H_jH_{3-j}\overline{H}_{3-j} - b(1+\mathrm{i}\omega_j)^2(1-\mathrm{i}\omega_j)\mathrm{e}^{-\mathrm{i}\omega_j\sigma_c}H_j^2\overline{H}_j. \end{aligned}$$

The nonhomogeneous equation (27) has a solution if and only if the solvability conditions, $\langle g_1^*, n_1\rangle = 0$ and $\langle g_2^*, n_2\rangle = 0$, are satisfied, where g_j^* $(j = 1, 2)$ is given by (23). Then $\frac{\partial H_1}{\partial T_1}$ and $\frac{\partial H_2}{\partial T_1}$ are solved to yield

$$\begin{aligned} \frac{\partial H_1}{\partial T_1} &= \eta_1H_1 + \eta_3H_1^2\overline{H}_1 + \eta_5H_1H_2\overline{H}_2, \\ \frac{\partial H_2}{\partial T_1} &= \eta_2H_2 + \eta_4H_2^2\overline{H}_2 + \eta_6H_1\overline{H}_1H_2, \end{aligned} \tag{28}$$

where

$$\eta_j = -\frac{\mathrm{i}\omega_j(1+\mathrm{i}\omega_j)\mathrm{e}^{-\mathrm{i}\omega_j\tau_c}a\tau_\epsilon + \mathrm{i}(1+\mathrm{i}\omega_j)^2b\sigma_\epsilon\omega_j\mathrm{e}^{-\mathrm{i}\omega_j\sigma_c}}{2(1+\mathrm{i}\omega_j)^3 + a\mathrm{e}^{-\mathrm{i}\omega_j\tau_c} + a\tau_c\mathrm{e}^{-\mathrm{i}\omega_j\tau_c}(1+\mathrm{i}\omega_j) + b\sigma_c\mathrm{e}^{-\mathrm{i}\omega_j\sigma_c}(1+\mathrm{i}\omega_j)^2}, \quad j = 1, 2,$$

$$\eta_3 = -\frac{(1+\mathrm{i}\omega_1)^4(1+\omega_1^2)(2+\omega_1^2) + a(1+\mathrm{i}\omega_1)\mathrm{e}^{-\mathrm{i}\omega_1\tau_c}}{2(1+\mathrm{i}\omega_1)^3 + a\mathrm{e}^{-\mathrm{i}\omega_1\tau_c} + a\tau_c\mathrm{e}^{-\mathrm{i}\omega_1\tau_c}(1+\mathrm{i}\omega_1) + b\sigma_c\mathrm{e}^{-\mathrm{i}\omega_1\sigma_c}(1+\mathrm{i}\omega_1)^2},$$

$$\eta_4 = -\frac{(1+\mathrm{i}\omega_2)^4(1+\omega_2^2)(2+\omega_2^2) + a(1+\mathrm{i}\omega_2)\mathrm{e}^{-\mathrm{i}\omega_2\tau_c}}{2(1+\mathrm{i}\omega_2)^3 + a\mathrm{e}^{-\mathrm{i}\omega_2\tau_c} + a\tau_c\mathrm{e}^{-\mathrm{i}\omega_2\tau_c}(1+\mathrm{i}\omega_2) + b\sigma_c\mathrm{e}^{-\mathrm{i}\omega_2\sigma_c}(1+\mathrm{i}\omega_2)^2}, \tag{29}$$

$$\eta_5 = -\frac{2(1+\mathrm{i}\omega_1)^4(1+\omega_2^2)(2+\omega_2^2) + 2a(1+\mathrm{i}\omega_1)\mathrm{e}^{-\mathrm{i}\omega_1\tau_c}}{2(1+\mathrm{i}\omega_1)^3 + a\mathrm{e}^{-\mathrm{i}\omega_1\tau_c} + a\tau_c\mathrm{e}^{-\mathrm{i}\omega_1\tau_c}(1+\mathrm{i}\omega_1) + b\sigma_c\mathrm{e}^{-\mathrm{i}\omega_1\sigma_c}(1+\mathrm{i}\omega_1)^2},$$

$$\eta_6 = -\frac{2(1+\mathrm{i}\omega_2)^4(1+\omega_1^2)(2+\omega_1^2) + 2a(1+\mathrm{i}\omega_2)\mathrm{e}^{-\mathrm{i}\omega_2\tau_c}}{2(1+\mathrm{i}\omega_2)^3 + a\mathrm{e}^{-\mathrm{i}\omega_2\tau_c} + a\tau_c\mathrm{e}^{-\mathrm{i}\omega_2\tau_c}(1+\mathrm{i}\omega_2) + b\sigma_c\mathrm{e}^{-\mathrm{i}\omega_2\sigma_c}(1+\mathrm{i}\omega_2)^2}.$$

Eq. (28) is the normal form truncated at the cubic order terms associated with the double Hopf bifurcation at the critical point: $\tau = \tau_c$ and $\sigma = \sigma_c$. Substituting $H_j = r_j\mathrm{e}^{\mathrm{i}\theta_j}$ $(j = 1, 2)$ into (28), yields the following normal form in polar coordinates:

$$\begin{aligned} \frac{\mathrm{d}r_1}{\mathrm{d}t} &= \beta_1r_1 + A_1r_1^3 + A_2r_1r_2^2, \\ \frac{\mathrm{d}r_2}{\mathrm{d}t} &= \beta_2r_2 + A_3r_2^3 + A_4r_2r_1^2, \\ \frac{\mathrm{d}\theta_1}{\mathrm{d}t} &= \beta_3 + A_5r_1^2 + A_6r_2^2, \\ \frac{\mathrm{d}\theta_1}{\mathrm{d}t} &= \beta_4 + A_7r_2^2 + A_8r_1^2, \end{aligned} \tag{30}$$

where $\beta_1 = \mathrm{Re}(\eta_1)$, $\beta_2 = \mathrm{Re}(\eta_2)$ $\beta_3 = \mathrm{Im}(\eta_1)$, $\beta_4 = \mathrm{Im}(\eta_2)$, $A_1 = \mathrm{Re}(\eta_3)$, $A_2 = \mathrm{Re}(\eta_5)$, $A_3 = \mathrm{Re}(\eta_4)$, $A_4 = \mathrm{Re}(\eta_6)$, $A_5 = \mathrm{Im}(\eta_3)$, $A_6 = \mathrm{Im}(\eta_5)$, $A_7 = \mathrm{Im}(\eta_4)$, $A_8 = \mathrm{Im}(\eta_6)$, and $\eta_i's$ $(i = 1, 2, 3, \ldots, 6)$ are given in (29).

4.2. Resonant case

In this subsection, we consider resonant double Hopf bifurcation. Suppose $\pm\mathrm{i}\omega_1$ and $\pm\mathrm{i}\omega_2$ are the eigenvalues of the linear operator $\widetilde{L}_c$, where $\omega_1 : \omega_2 = l_1\omega_0 : l_2\omega_0$ with l_1/l_2 rational.

Theorem 4.1. *The normal forms of system (13) for resonant cases are different from that of the non-resonant case, with only two possibilities of the ratio $l_1 : l_2$, either $1:3$ or $3:1$.*

Proof. The normal form of (13) is obtained by eliminating the secular terms in the linear part of the ordered perturbation equations. Hence, we need only consider the nonlinear terms $-\frac{1}{3}\left(u_2^{(1)}(T_0,T_1)\right)^3$, $-\frac{1}{3}\left(u_3^{(1)}(T_0,T_1)\right)^3$, $-\frac{a}{3}\left(u_1^{(1)}(T_0-\tau_c,T_1)\right)^3$ and $-\frac{b}{3}\left(u_2^{(1)}(T_0-\sigma_c,T_1)\right)^3$. Combining all products and powers of trigonometric terms into a sum of trigonometric terms shows that only the following terms may produce the secular terms,

$$\mathrm{e}^{\pm(2\varphi-\psi)T_0} \quad \text{and} \quad \mathrm{e}^{\pm 3\varphi T_0},$$

where $\varphi,\ \psi = l_i\omega_0 T_0,\ i = 1,2$. It is easy to see that a secular term may occur only if $l_1 : l_2 = 1:3$ or $l_1 : l_2 = 3:1$. The proof is complete. □

Similar to the non-resonant case, suppose $\pm\mathrm{i}\omega_0$ and $\pm 3\mathrm{i}\omega_0$ are the eigenvalues of the linear operator $\widetilde{L}_c$. Then the solution of (24) can be expressed in the form of

$$u^{(1)}(T_0,T_1,T_2) = K_1(T_1,T_2)q_1\mathrm{e}^{\mathrm{i}\omega_0 T_0} + \overline{K}_1(T_1,T_2)\bar{q}_1\mathrm{e}^{-\mathrm{i}\omega_0 T_0} + K_2(T_1,T_2)q_2\mathrm{e}^{3\mathrm{i}\omega_0 T_0} + \overline{K}_2(T_1,T_2)\bar{q}_2\mathrm{e}^{-3\mathrm{i}\omega_0 T_0}, \tag{31}$$

where

$$q_j = (q_{j1}, q_{j2}, q_{j3})^{\mathrm{T}} = (1, 1+\mathrm{i}\omega_j, (1+\mathrm{i}\omega_j)^2)^{\mathrm{T}}, \quad j = 1,2, \tag{32}$$

with $\omega_1 = \omega_0$ and $\omega_2 = 3\omega_0$.

Substituting solution (31) into (26) and simplifying, we can obtain a linear nonhomogeneous equation for $u^{(2)}$:

$$\mathrm{D}_0 u^{(2)} - M_1 u^{(2)} - aM_2 u_{\tau_c}^{(2)} - bM_3 u_{\sigma_c}^{(2)} = p_1\mathrm{e}^{\mathrm{i}\omega_0 T_0} + \bar{p}_1\mathrm{e}^{-\mathrm{i}\omega_0 T_0} + p_2\mathrm{e}^{3\mathrm{i}\omega_0 T_0} + \bar{p}_2\mathrm{e}^{-3\mathrm{i}\omega_0 T_0}, \tag{33}$$

where $p_j = \left(p_j^{(1)}, p_j^{(2)}, p_j^{(3)}\right)^{\mathrm{T}}$ with

$$p_1^{(1)} = -\frac{\partial K_1}{\partial T_1} - (1+\mathrm{i}\omega_0)^2(1-\mathrm{i}\omega_0)K_1^2\overline{K}_1 - 2(1+\mathrm{i}\omega_0)(1+3\mathrm{i}\omega_0)(1-3\mathrm{i}\omega_0)K_1K_2\overline{K}_2 - (1-\mathrm{i}\omega_0)^2(1+3\mathrm{i}\omega_0)\overline{K}_1^2K_2,$$

$$p_2^{(1)} = -\frac{\partial K_2}{\partial T_1} - (1+3\mathrm{i}\omega_0)^2(1-3\mathrm{i}\omega_0)K_2^2\overline{K}_2 - 2(1+\mathrm{i}\omega_0)(1-\mathrm{i}\omega_0)(1+3\mathrm{i}\omega_0)K_2K_1\overline{K}_1 - \frac{1}{3}(1+\mathrm{i}\omega_0)^3K_1^3,$$

$$\begin{aligned} p_1^{(2)} = {} & -(1+\mathrm{i}\omega_0)\frac{\partial K_1}{\partial T_1} - 2(1+\mathrm{i}\omega_0)^2(1+3\mathrm{i}\omega_0)^2(1-3\mathrm{i}\omega_0)^2K_1K_2\overline{K}_2 - (1+\mathrm{i}\omega_0)^4(1-\mathrm{i}\omega_0)^2K_1^2\overline{K}_1 \\ & - (1-\mathrm{i}\omega_0)^4(1+3\mathrm{i}\omega_0)^2\overline{K}_1^2K_2, \end{aligned}$$

$$p_2^{(2)} = -(1+3\mathrm{i}\omega_0)\frac{\partial K_2}{\partial T_1} - 2(1+\mathrm{i}\omega_0)^2(1-\mathrm{i}\omega_0)^2(1+3\mathrm{i}\omega_0)^2K_1\overline{K}_1K_2 - (1+3\mathrm{i}\omega_0)^4(1-3\mathrm{i}\omega_0)^2K_2^2\overline{K}_2 - \frac{1}{3}(1+\mathrm{i}\omega_0)^6K_1^3,$$

$$\begin{aligned} p_1^{(3)} = {} & -\frac{\partial K_1}{\partial T_1}(1+\mathrm{i}\omega_0)^2 - \mathrm{i}\omega_0 a\tau_\epsilon K_1\mathrm{e}^{-\mathrm{i}\omega_0\tau_c} - a\tau_c\frac{\partial K_1}{\partial T_1}\mathrm{e}^{-\mathrm{i}\omega_0\tau_c} \\ & - b\sigma_\epsilon(1+\mathrm{i}\omega_0)\mathrm{i}\omega_0K_1\mathrm{e}^{-\mathrm{i}\omega_0\sigma_c} - b\sigma_c(1+\mathrm{i}\omega_0)\mathrm{e}^{-\mathrm{i}\omega_0\sigma_c}\frac{\partial K_1}{\partial T_1} - 2a\mathrm{e}^{-\mathrm{i}\omega_0\tau_c}K_1K_2\overline{K}_2 - a\mathrm{e}^{-\mathrm{i}\omega_0\tau_c}K_1^2\overline{K}_1 \\ & - a\mathrm{e}^{-\mathrm{i}\omega_0\tau_c}\overline{K}_1^2K_2 - 2b(1+\mathrm{i}\omega_0)(1+3\mathrm{i}\omega_0)(1-3\mathrm{i}\omega_0)\mathrm{e}^{-\mathrm{i}\omega_0\sigma_c}K_1K_2\overline{K}_2 \\ & - b(1+\mathrm{i}\omega_0)^2(1-\mathrm{i}\omega_0)\mathrm{e}^{-\mathrm{i}\omega_0\sigma_c}K_1^2\overline{K}_1 - b(1-\mathrm{i}\omega_0)^2(1+3\mathrm{i}\omega_0)\mathrm{e}^{-\mathrm{i}\omega_0\sigma_c}\overline{K}_1^2K_2, \end{aligned}$$

$$\begin{aligned} p_2^{(3)} = {} & -\frac{\partial K_2}{\partial T_1}(1+3\mathrm{i}\omega_0)^2 - 3\mathrm{i}\omega_0 a\tau_\epsilon K_2\mathrm{e}^{-3\mathrm{i}\omega_0\tau_c} - a\tau_c\frac{\partial K_2}{\partial T_1}\mathrm{e}^{-3\mathrm{i}\omega_0\tau_c} - 3b\sigma_\epsilon(1+3\mathrm{i}\omega_0)\mathrm{i}\omega_0K_2\mathrm{e}^{-3\mathrm{i}\omega_0\sigma_c} \\ & - b\sigma_c(1+3\mathrm{i}\omega_0)\mathrm{e}^{-3\mathrm{i}\omega_0\sigma_c}\frac{\partial K_2}{\partial T_1} - 2a\mathrm{e}^{-3\mathrm{i}\omega_0\tau_c}K_1\overline{K}_1K_2 - a\mathrm{e}^{-3\mathrm{i}\omega_0\tau_c}K_2^2\overline{K}_2 \\ & - \frac{a}{3}\mathrm{e}^{-3\mathrm{i}\omega_0\tau_c}K_1^3 - 2b(1+\mathrm{i}\omega_0)(1-\mathrm{i}\omega_0)(1+3\mathrm{i}\omega_0)\mathrm{e}^{-3\mathrm{i}\omega_0\sigma_c}K_1\overline{K}_1K_2 \\ & - b(1+3\mathrm{i}\omega_0)^2(1-3\mathrm{i}\omega_0)\mathrm{e}^{-3\mathrm{i}\omega_0\sigma_c}K_2^2\overline{K}_2 - \frac{b}{3}(1+\mathrm{i}\omega_0)^3\mathrm{e}^{-3\mathrm{i}\omega_0\sigma_c}K_1^3. \end{aligned}$$

The nonhomogeneous equation (33) has a solution if and only if the solvability conditions, $\langle q_1^*, p_1\rangle = 0$ and $\langle q_2^*, p_2\rangle = 0$ are satisfied, where

$$q_j^* = (q_{j1}^*, q_{j2}^*, q_{j3}^*) = \left(\frac{a e^{i\omega_j \tau_c}}{2(1-i\omega_j)^3 + a e^{i\omega_j \tau_c}}, \frac{(1-i\omega_j)^2}{2(1-i\omega_j)^3 + a e^{i\omega_j \tau_c}}, \frac{1-i\omega_j}{2(1-i\omega_j)^3 + a e^{i\omega_j \tau_c}} \right), \quad j = 1, 2.$$

These two equations are used to solve for $\frac{\partial K_1}{\partial T_1}$ and $\frac{\partial K_2}{\partial T_1}$ to obtain

$$\begin{aligned} \frac{\partial K_1}{\partial T_1} &= \xi_1 K_1 + \xi_2 K_1^2 \overline{K}_1 + \xi_3 K_1 K_2 \overline{K}_2 + \xi_4 \overline{K}_1^2 K_2, \\ \frac{\partial K_2}{\partial T_1} &= \xi_5 K_2 + \xi_6 K_2^2 \overline{K}_2 + \xi_7 K_1 \overline{K}_1 K_2 + \xi_8 K_1^3, \end{aligned} \tag{34}$$

where

$$\begin{aligned} \xi_1 &= -\frac{i\omega_0(1+i\omega_0)e^{-i\omega_0\tau_c} a\tau_\epsilon + i(1+i\omega_0)^2 b\sigma_\epsilon \omega_0 e^{-i\omega_0\sigma_c}}{2(1+i\omega_0)^3 + a e^{-i\omega_0\tau_c} + a\tau_c e^{-i\omega_0\tau_c}(1+i\omega_0) + b\sigma_c e^{-i\omega_0\sigma_c}(1+i\omega_0)^2}, \\ \xi_2 &= -\frac{(1+i\omega_0)^4(1+\omega_0^2)(2+\omega_0^2) + a(1+i\omega_0)e^{-i\omega_0\tau_c}}{2(1+i\omega_0)^3 + a e^{-i\omega_0\tau_c} + a\tau_c e^{-i\omega_0\tau_c}(1+i\omega_0) + b\sigma_c e^{-i\omega_0\sigma_c}(1+i\omega_0)^2}, \\ \xi_3 &= -\frac{2(1+i\omega_0)^4(1+9\omega_0^2)(2+9\omega_0^2) + 2a(1+i\omega_0)e^{-i\omega_0\tau_c}}{2(1+i\omega_0)^3 + a e^{-i\omega_0\tau_c} + a\tau_c e^{-i\omega_0\tau_c}(1+i\omega_0) + b\sigma_c e^{-i\omega_0\sigma_c}(1+i\omega_0)^2}, \\ \xi_4 &= -\frac{(1-i\omega_0)^2(1+3i\omega_0)(1+i\omega_0)^3 + (1+i\omega_0)^2(1-i\omega_0)^4(1+3i\omega_0)^2 + a(1+i\omega_0)e^{-i\omega_0\tau_c}}{2(1+i\omega_0)^3 + a e^{-i\omega_0\tau_c} + a\tau_c e^{-i\omega_0\tau_c}(1+i\omega_0) + b\sigma_c e^{-i\omega_0\sigma_c}(1+i\omega_0)^2}, \\ \xi_5 &= -\frac{3i\omega_0(1+3i\omega_0)e^{-3i\omega_0\tau_c} a\tau_\epsilon + 3i(1+3i\omega_0)^2 b\sigma_\epsilon \omega_0 e^{-3i\omega_0\sigma_c}}{2(1+3i\omega_0)^3 + a e^{-3i\omega_0\tau_c} + a\tau_c e^{-3i\omega_0\tau_c}(1+3i\omega_0) + b\sigma_c e^{-3i\omega_0\sigma_c}(1+3i\omega_0)^2}, \\ \xi_6 &= -\frac{(1+3i\omega_0)^4(1+9\omega_0^2)(2+9\omega_0^2) + a(1+3i\omega_0)e^{-3i\omega_0\tau_c}}{2(1+3i\omega_0)^3 + a e^{-3i\omega_0\tau_c} + a\tau_c e^{-3i\omega_0\tau_c}(1+3i\omega_0) + b\sigma_c e^{-3i\omega_0\sigma_c}(1+3i\omega_0)^2}, \\ \xi_7 &= -\frac{2(1+3i\omega_0)^4(1+\omega_0^2)(2+\omega_0^2) + 2a(1+3i\omega_0)e^{-3i\omega_0\tau_c}}{2(1+3i\omega_0)^3 + a e^{-3i\omega_0\tau_c} + a\tau_c e^{-3i\omega_0\tau_c}(1+3i\omega_0) + b\sigma_c e^{-3i\omega_0\sigma_c}(1+3i\omega_0)^2}, \\ \xi_8 &= -\frac{(1+i\omega_0)^3(1+3i\omega_0)^3 + (1+3i\omega_0)^2(1+i\omega_0)^6 + a(1+3i\omega_0)e^{-3i\omega_0\tau_c}}{3[2(1+3i\omega_0)^3 + a e^{-3i\omega_0\tau_c} + a\tau_c e^{-3i\omega_0\tau_c}(1+3i\omega_0) + b\sigma_c e^{-3i\omega_0\sigma_c}(1+3i\omega_0)^2]}. \end{aligned} \tag{35}$$

Eq. (34) is the normal form truncated at the cubic order terms associated with the resonant double Hopf bifurcation at the critical point: $\tau = \tau_c$ and $\sigma = \sigma_c$. Substituting $K_j = R_j e^{i\Theta_j}$ $(j = 1, 2)$ into (34), yields the following normal form in polar coordinates:

$$\begin{aligned} \frac{dR_1}{dt} &= \mathrm{Re}(\xi_1)R_1 + \mathrm{Re}(\xi_2)R_1^3 + \mathrm{Re}(\xi_3)R_1R_2^2 + \mathrm{Re}(\xi_4)R_1^2R_2\cos(\Phi) + \mathrm{Im}(\xi_4)R_1^2R_2\sin(\Phi), \\ \frac{dR_2}{dt} &= \mathrm{Re}(\xi_5)R_2 + \mathrm{Re}(\xi_6)R_2^3 + \mathrm{Re}(\xi_7)R_2R_1^2 + \mathrm{Re}(\xi_8)R_1^3\cos(\Phi) - \mathrm{Im}(\xi_8)\sin(\Phi)R_1^3, \\ \frac{d\Theta_1}{dt} &= \mathrm{Im}(\xi_1) + \mathrm{Im}(\xi_2)R_1^2 + \mathrm{Im}(\xi_3)R_2^2 + \mathrm{Im}(\xi_4)R_1R_2\cos(\Phi) - \mathrm{Re}(\xi_4)\sin(\Phi)R_1R_2, \\ R_2\frac{d\Theta_1}{dt} &= \mathrm{Im}(\xi_5)R_2 + \mathrm{Im}(\xi_6)R_2^3 + \mathrm{Im}(\xi_7)R_1^2R_2 + \mathrm{Im}(\xi_8)\cos(\Phi)R_1^3 + \mathrm{Re}(\xi_8)\sin(\Phi)R_1^3, \end{aligned} \tag{36}$$

where $\Phi = 3\Theta_1 - \Theta_2$ and $\xi_i' s$ $(i = 1, 2, 3, \ldots, 8)$ are given in (35).

5. Bifurcation analysis and numerical simulation

In this section, we first study Hopf-zero bifurcation and then double Hopf bifurcation.

5.1. Hopf-zero bifurcation

The bifurcation analysis is given based on the first two equations of the normal form (22), and then some numerical simulation results are presented. Consider the following equations,

$$\begin{aligned}\frac{dr}{dt} &= \alpha_1 r + J_1 r^3 + J_2 r z^2,\\ \frac{dz}{dt} &= \alpha_2 z + J_3 z^3 + J_4 z r^2,\end{aligned} \tag{37}$$

which are the first two equations of (22).

The equilibrium solutions of (37) are obtained by simply setting $\frac{dr}{dt} = \frac{dz}{dt} = 0$. Note that $E_0 = (r,z) = (0,0)$ corresponds to the original trivial equilibrium, and the other ones are

$$E_1 = \left(\sqrt{-\frac{\alpha_1}{J_1}}, 0\right) \quad \text{for } \frac{\alpha_1}{J_1} < 0,$$

$$E_2^{\pm} = \left(0, \pm\sqrt{-\frac{\alpha_2}{J_3}}\right) \quad \text{for } \frac{\alpha_2}{J_3} < 0,$$

$$E_3^{\pm} = \left(\sqrt{\frac{\alpha_2 J_2 - \alpha_1 J_3}{J_1 J_3 - J_2 J_4}}, \pm\sqrt{\frac{\alpha_2 J_1 - \alpha_1 J_4}{J_2 J_4 - J_1 J_3}}\right) \quad \text{for } \frac{\alpha_2 J_2 - \alpha_1 J_3}{J_1 J_3 - J_2 J_4} > 0, \quad \frac{\alpha_2 J_1 - \alpha_1 J_4}{J_2 J_4 - J_1 J_3} > 0.$$

The semi-trivial equilibria E_1 and $E_2^{\pm}$ bifurcate from the origin on the critical lines $L_1 : \alpha_1 = 0$ and $L_2 : \alpha_2 = 0$, respectively. The pair of nontrivial equilibria $E_3^{\pm}$ collide with the semi-trivial equilibria $E_2^{\pm}$ and E_1 respectively on the critical lines $L_3 : \alpha_2 J_2 - \alpha_1 J_3 = 0$ and $L_4 : \alpha_2 J_1 - \alpha_1 J_4 = 0$.

When $(a,\sigma) = (a_c,\sigma_c)$, the solutions on the center manifold determine the local asymptotic behavior of solutions of the original system (2). So, the equilibria of system (2) on the z–axis remain equilibria, while equilibria away from the z–axis are actually periodic orbits (with period $\approx 2\pi/\omega$).

To give a more clear bifurcation picture, we choose $a = -1$ and $b = 2$, which satisfy the assumption of Theorem 2.3. When $a = -1$ and $b = 2$, Eq. (6) has no positive root. By Lemma 2.1, all roots of Eq. (4) have negative real part for all $\tau \geqslant 0$. We choose $\tau = 2$, for which (10) has only one positive root, $\omega = 1.029013154$, and we, by (11) and (12), obtain $\sigma^{(0)} = 4.217519765$ and $\mathrm{Re}(\lambda'(\sigma^{(0)})) > 0$. Therefore, by Theorem 2.3, when $a = -1$, $b = 2$, $\tau = 2$ and $\sigma = 4.217519765$, the characteristic Eq. (3) has a zero and a pair of purely imaginary eigenvalues $\pm i\omega = \pm 1.029013154i$, and all the other eigenvalues have negative real part, implying that system (2) undergoes a Hopf-zero bifurcation. By a simple calculation, we obtain $\alpha_1 = 0.0870727357\sigma_\epsilon - 0.02384068405a_\epsilon$, $\alpha_2 = 0.1344982762a_\epsilon$, $J_1 = -1.302977187$, $J_2 = -0.4300572437$, $J_3 = -0.04483275872$ and $J_4 = -1.425091496$.

For the above chosen parameter values, the critical bifurcation lines become: $L_1 : \sigma_\epsilon = 0.2738019411a_\epsilon$, $L_2 : a_\epsilon = 0$, $L_3 : \sigma_\epsilon = 15.09097429a_\epsilon$, $L_4 : \sigma_\epsilon = 1.686107251a_\epsilon$, as shown in the bifurcation diagram (see Fig. 2).

Fig. 2 shows the critical bifurcation lines in the $(a_\epsilon,\sigma_\epsilon)$ parameter plane near the critical point (a_c,σ_c), and the corresponding phase portraits in the (r,z) plane, whose origin is the Hopf-zero bifurcation critical point. The bifurcation behaviors of the original system (2) in the neighborhood of $(0,0,0)$ can be observed from Fig. 2. Note that the bifurcation boundaries divide the $(a_\epsilon,\sigma_\epsilon)$ parameter plane into six regions. Also, it is seen from the phase portraits that the orbits are symmetric with respect to the r–coordinate, therefore, we only draw the orbits in the first quadrant.

For system (2), we use Fig. 2 to describe the bifurcations in the clockwise direction, starting from C_1 and ending at C_1. First, in region C_1, there is only one trivial equilibrium which is a sink. When the parameters are varied across the line L_1 from region C_1 to C_2, the trivial equilibrium becomes a saddle, and a stable periodic solution (for convenience, we call it S_1) appears from the trivial solution due to a Hopf bifurcation. When the parameters are changed from region C_2 to C_3, a pair of unstable fixed points (called $S_2^{\pm}$) occur from the trivial solution due to a pitchfork bifurcation, while the trivial fixed point becomes a source from a saddle. In region C_4, a pair of periodic solutions (called $S_3^{\pm}$), which are sources, occur from $S_2^{\pm}$ due to a pitchfork bifurcation, and $S_2^{\pm}$ become sinks from saddles. When the parameters are further changed from region C_4 to C_5 crossing the line L_4, the pair of periodic solutions $S_3^{\pm}$ collide with the periodic solution S_1, and then disappear, and S_1 becomes saddle. When the parameters are further varied across the line L_1 from region C_5 to C_6, the periodic solution S_1 collides with the trivial solution and then disappears, and the trivial solution becomes a saddle from a source. Finally, when the parameters are varied across the line L_2 (the σ_ϵ axis) from region C_6 to C_1, the pair of stable fixed points $S_2^{\pm}$ collide with the trivial solution and then disappear, and the trivial solution becomes a sink from a saddle.

For simulations, we choose four groups of perturbation parameter values: $(a_\epsilon,\sigma_\epsilon) = (-0.01,-0.1), (0.05,0.9)$, (0.1,0.8) and (0.1,−0.1), which belong to the regions C_1, C_3, C_4 and C_6, respectively, resulting in a stable fixed point shown in Fig. 3, a stable periodic solution as depicted in Fig. 4, coexistence of a pair of stable fixed points and a stable periodic solution shown in Fig. 5, and a pair of stable fixed points as depicted in Fig. 6. It is clear that the numerical simulations agree with the analytical predictions.

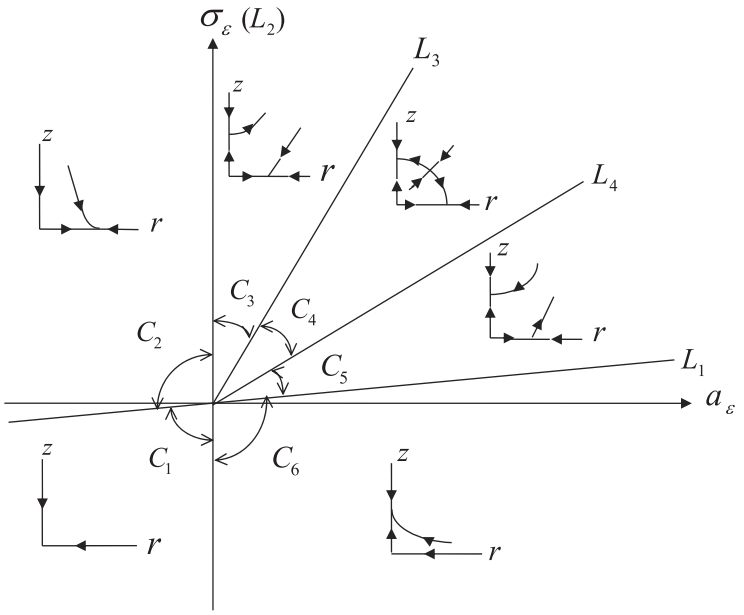

Fig. 2. Critical bifurcation lines in the $(a_\epsilon, \sigma_\epsilon)$ parameter plane near the Hopf-zero critical point (a_c, σ_c) and the corresponding phase portraits in the (r, z) plane.

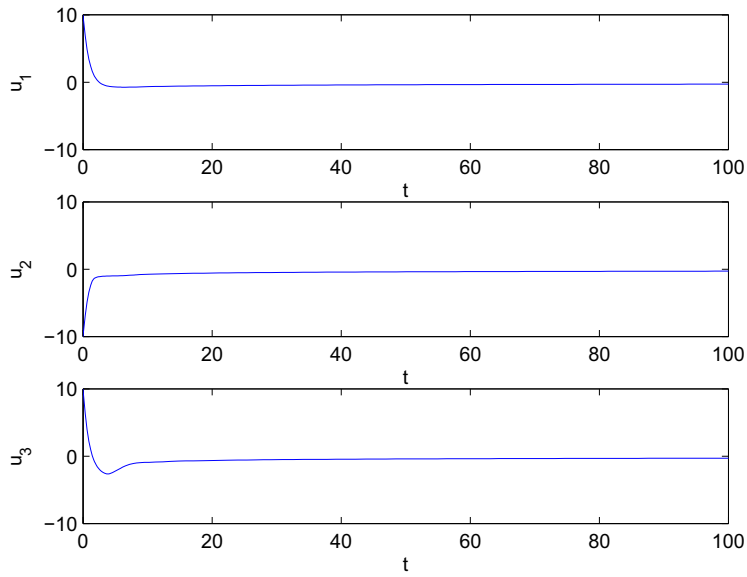

Fig. 3. Simulated solution of system (2) associated with the Hopf-zero bifurcation, for $(a_c, \sigma_c) = (-1, 4.217519765)$, $b = 2$, $\tau = 2$ and $(a_\epsilon, \sigma_\epsilon) = (-0.01, -0.1)$, showing a stable fixed point.

5.2. Non-resonant double Hopf bifurcation

In this subsection, we first give a bifurcation analysis based on the first two equations of the normal form (30), and then present some numerical simulation results. Consider the following equations,

$$\begin{aligned} \frac{dr_1}{dt} &= \beta_1 r_1 + A_1 r_1^3 + A_2 r_1 r_2^2, \\ \frac{dr_2}{dt} &= \beta_2 r_2 + A_3 r_2^3 + A_4 r_2 r_1^2, \end{aligned} \tag{38}$$

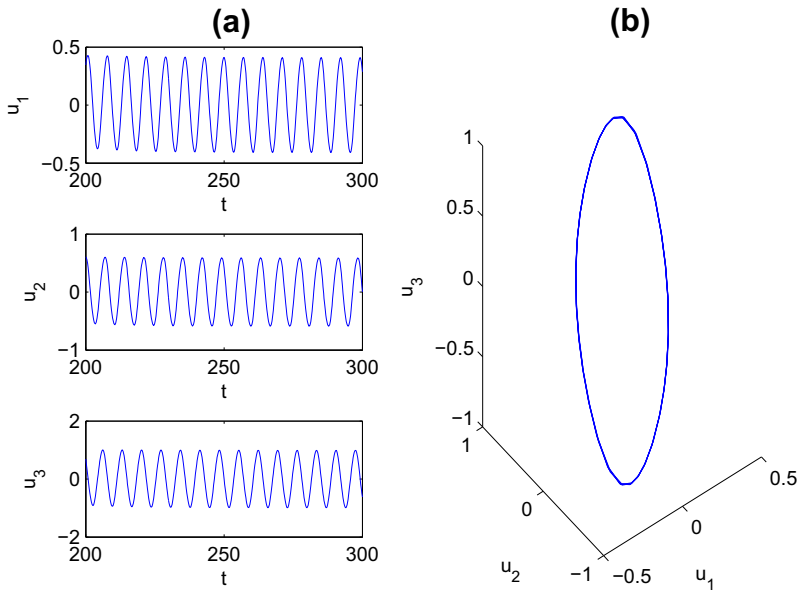

Fig. 4. Simulated solution of system (2) associated with the Hopf-zero bifurcation, for $(a_\epsilon, \sigma_\epsilon) = (-1, 4.217519765)$, $b = 2$, $\tau = 2$ and $(a_\epsilon, \sigma_\epsilon) = (0.05, 0.9)$: (a) the time history; and (b) the phase portrait, showing a stable periodic solution.

which are actually first two equations of (30).

The equilibrium solutions of (38) are obtained by simply setting $\frac{dr_1}{dt} = \frac{dr_2}{dt} = 0$. Note that $F_0 = (r_1, r_2) = (0, 0)$ corresponds to the original trivial equilibrium, and the other ones are

$$F_1 = \left(\sqrt{-\frac{\beta_1}{A_1}}, 0\right) \quad \text{for } \frac{\beta_1}{A_1} < 0,$$

$$F_2 = \left(0, \sqrt{-\frac{\beta_2}{A_3}}\right) \quad \text{for } \frac{\beta_2}{A_3} < 0,$$

$$F_3 = \left(\sqrt{\frac{\beta_2 A_2 - \beta_1 A_3}{A_1 A_3 - A_2 A_4}}, \sqrt{\frac{\beta_2 A_1 - \beta_1 A_4}{A_2 A_4 - A_1 A_3}}\right) \quad \text{for } \frac{\beta_2 A_2 - \beta_1 A_3}{A_1 A_3 - A_2 A_4} > 0, \quad \frac{\beta_2 A_1 - \beta_1 A_4}{A_2 A_4 - A_1 A_3} > 0.$$

The semi-trivial equilibria F_1 and F_2 bifurcate from the origin on the critical lines $L_1 : \beta_1 = 0$ and $L_2 : \beta_2 = 0$, respectively. The nontrivial equilibrium F_3 collides with the semi-trivial equilibria F_2 and F_1 respectively on the critical lines $L_3 : \beta_2 A_2 - \beta_1 A_3 = 0$ and $L_4 : \beta_2 A_1 - \beta_1 A_4 = 0$.

We choose $a = -1$ and $b = -1.485451766$, for which all roots of (4) with $\tau = 0$ have negative real part, and Eq. (6) has no positive root. By Lemma 2.1, all roots of Eq. (4) have negative real part for all $\tau \geqslant 0$. Let $\omega_1 : \omega_2 = \frac{l_1}{l_2} = \frac{\sqrt{2}}{2}$. Then, choose $\tau = 13.16190556$, under which the positive roots $\tilde{\omega}_k$ of (10), the time delay $\sigma_k^{(0,1)}$ $(k = 1, 2, \ldots, 6)$ and the transversality conditions are given as follows:

$$\begin{aligned}
&\tilde{\omega}_1 = 0.009112379716, \quad \sigma_1^{(0)} = 40.49677901, \quad \mathrm{Re}(\lambda'(\sigma_1^{(0)})) < 0,\\
&\tilde{\omega}_2 = 0.2961901579, \quad \sigma_2^{(0)} = 6.296902204, \quad \mathrm{Re}(\lambda'(\sigma_2^{(0)})) > 0,\\
&\tilde{\omega}_3 = 0.4967403723, \quad \sigma_3^{(0)} = 5.767516314, \quad \mathrm{Re}(\lambda'(\sigma_3^{(0)})) < 0,\\
&\tilde{\omega}_4 = 0.6797869345, \quad \sigma_4^{(0)} = 2.028520562, \quad \mathrm{Re}(\lambda'(\sigma_4^{(0)})) > 0,\\
&\tilde{\omega}_5 = 0.9613639020, \quad \sigma_5^{(0)} = 2.028520562, \quad \mathrm{Re}(\lambda'(\sigma_5^{(0)})) < 0,\\
&\tilde{\omega}_6 = 1.042353940, \quad \sigma_6^{(0)} = 1.279687398, \quad \sigma_6^{(1)} = 7.307568204, \quad \mathrm{Re}(\lambda'(\sigma_6^{(0,1)})) > 0.
\end{aligned}$$

Therefore, when $a = -1$, $b = -1.485451766$, $\tau = 13.16190556$ and $\sigma = 2.028520562$, the characteristic Eq. (3) has two pairs of purely imaginary eigenvalues $\pm i\omega_1 = \pm i\tilde{\omega}_4 = \pm 0.6797869345i$ and $\pm i\omega_2 = \pm i\tilde{\omega}_5 = \pm 0.9613639020i$ with $\omega_1 : \omega_2 = \frac{\sqrt{2}}{2}$, and all the other eigenvalues have negative real part, and so system (2) undergoes a non-resonant double Hopf bifurcation.

Under the above chosen parameter values, by a simple calculation, we obtain

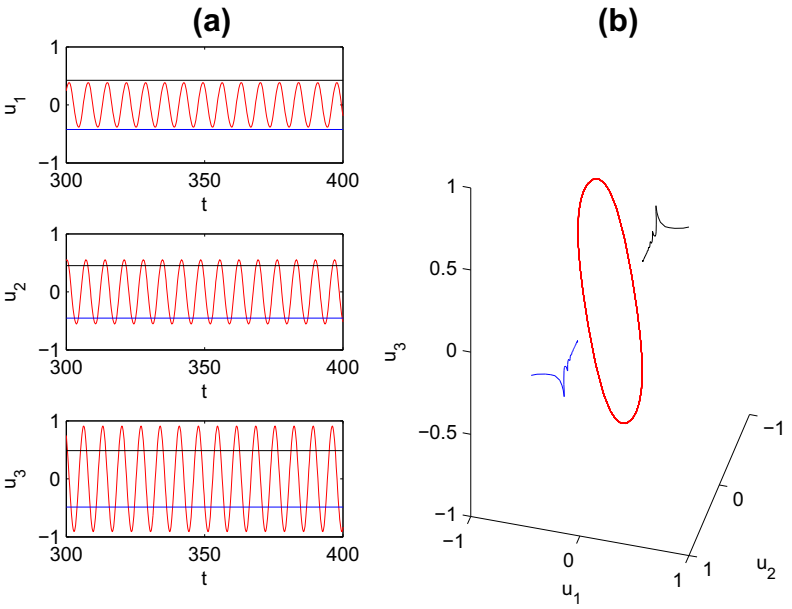

Fig. 5. Simulated solution of system (2) associated with the Hopf-zero bifurcation, for $(a_c, \sigma_c) = (-1, 4.217519765)$, $b = 2$, $\tau = 2$ and $(a_\epsilon, \sigma_\epsilon) = (0.1, 0.8)$: (a) the time history; and (b) the phase portrait, showing coexistence of a pair of stable fixed points with the initial values $(x_1(0), x_2(0), x_3(0)) = (1, 1, 1)$ (black lines) and $(x_1(0), x_2(0), x_3(0)) = (-1, -1, -1)$ (blue lines) and a stable periodic solution with the initial value $(x_1(0), x_2(0), x_3(0)) = (0.01, 0.01, 0.01)$ (red lines), respectively. (For interpretation of the references to colour in this figure legend, the reader is referred to the web version of this article.)

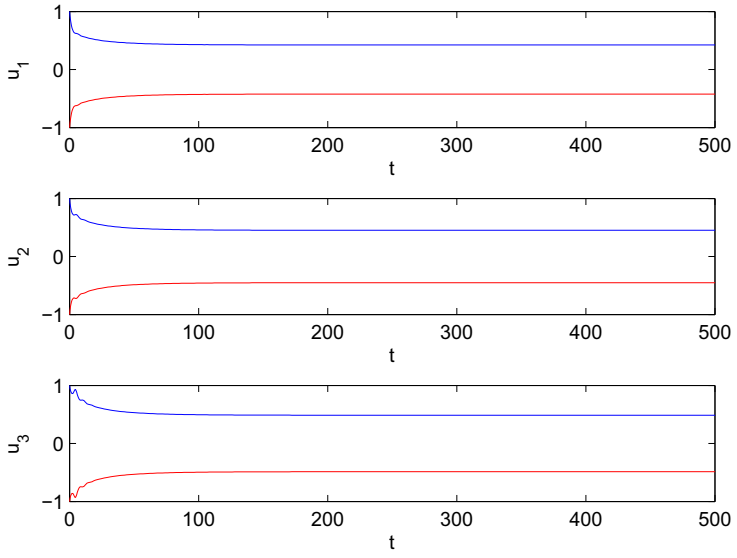

Fig. 6. Simulated solution of system (2) associated with the Hopf-zero bifurcation, for $(a_c, \sigma_c) = (-1, 4.217519765)$, $b = 2$, $\tau = 2$ and $(a_\epsilon, \sigma_\epsilon) = (0.1, -0.1)$, showing coexistence of a pair of stable fixed points with the initial values $(x_1(0), x_2(0), x_3(0)) = (1, 1, 1)$ (blue lines) and $(x_1(0), x_2(0), x_3(0)) = (-1, -1, -1)$ (red lines), respectively. (For interpretation of the references to colour in this figure legend, the reader is referred to the web version of this article.)

$$\beta_1 = 0.07764407970\sigma_\epsilon - 0.01353609245\tau_\epsilon, \quad \beta_2 = 0.02471039837\tau_\epsilon - 0.06541497668\sigma_\epsilon,$$
$$A_1 = -0.2807240645, \quad A_2 = -0.809569622, \quad A_3 = -0.864057456, \quad A_4 = -1.141808586.$$

The critical bifurcation lines become:

$$L_1 : \sigma_\epsilon = 0.1743351522\tau_\epsilon, \quad L_2 : \sigma_\epsilon = 0.3777483326\tau_\epsilon,$$
$$L_3 : \sigma_\epsilon = 0.2640696525\tau_\epsilon, \quad L_4 : \sigma_\epsilon = 0.2092393885\tau_\epsilon.$$

The bifurcation diagram is shown in Fig. 7. Fig. 7 shows the critical bifurcation lines in the $(\tau_\epsilon, \sigma_\epsilon)$ parameter plane near the critical point (τ_c, σ_c) and the corresponding phase portraits in the (r_1, r_2) plane, whose origin is the non-resonant double Hopf bifurcation critical point. The bifurcation behaviors of the original system (2) in the neighborhood of $(0,0,0)$ can be observed from Fig. 7. Note that the bifurcation boundaries divide the $(\tau_\epsilon, b_\epsilon)$ parameter plane into six regions (see Fig. 7).

For system (2), we use Fig. 7 to describe the bifurcations near the non-resonant double Hopf critical point in the clockwise direction, starting from B_1 and ending at B_1. First, in region B_1, there is only one trivial equilibrium which is a sink. When the parameters are varied across the line L_1 from region B_1 to B_2, the trivial equilibrium becomes a saddle, and a stable periodic solution (called O_1) appears from the trivial solution due to a Hopf bifurcation. When the parameters are changed from region B_2 to B_3, a unstable periodic solution (called O_2) occurs from the trivial solution due to a Hopf bifurcation, while the trivial fixed point becomes a source from a saddle. In region B_4, an unstable quasi-periodic solution occurs from O_2 due to a Neimark–Sacker bifurcation, and O_2 becomes a sink from a saddle. When the parameters are further changed from region B_4 to B_5 crossing the line L_4, the unstable quasi-periodic solution collides with the periodic solution O_1, and then disappears, and O_1 becomes a saddle. When the parameters are further varied across the line L_1 from region B_5 to B_6, O_1 collides with the trivial solution and then disappears, and the trivial solution becomes a saddle from a source. Finally, when the parameters are varied across the line L_2 from region B_6 to B_1, the stable periodic solution O_2 collides with the trivial solution and then disappears, and the trivial solution becomes a sink from a saddle.

We choose three groups of perturbation parameter values: $(\tau_\epsilon, \sigma_\epsilon) = (-0.1, -0.02)$, $(-0.1, 0.1)$, and $(0.1, 0.021)$, which belong to the regions B_1, B_2 and B_4, corresponding to a stable fixed point shown in Fig. 8, a stable periodic solution as depicted in Fig. 9, and coexistence of a pair of stable periodic solutions shown in Fig. 10, respectively. It is clear that the numerical simulations agree with the analytical predictions.

5.3. Resonant double Hopf bifurcation

In this subsection, we consider the normal form (36) associated with resonant double Hopf bifurcation. Note that $\widetilde{F}_0 = (R_1, R_2) = (0,0)$ is always the equilibrium solution of (36), which corresponds to the original trivial equilibrium, and the other semi-trivial equilibria of (36) are:

$$\widetilde{F}_1 = (R_1, R_2) = \left(\sqrt{-\frac{\mathrm{Re}(\xi_1)}{\mathrm{Re}(\xi_2)}}, 0\right), \quad \text{for } \frac{\mathrm{Re}(\xi_1)}{\mathrm{Re}(\xi_2)} < 0,$$

$$\widetilde{F}_2 = (R_1, R_2) = \left(0, \sqrt{-\frac{\mathrm{Re}(\xi_5)}{\mathrm{Re}(\xi_6)}}\right), \quad \text{for } \frac{\mathrm{Re}(\xi_5)}{\mathrm{Re}(\xi_6)} < 0.$$

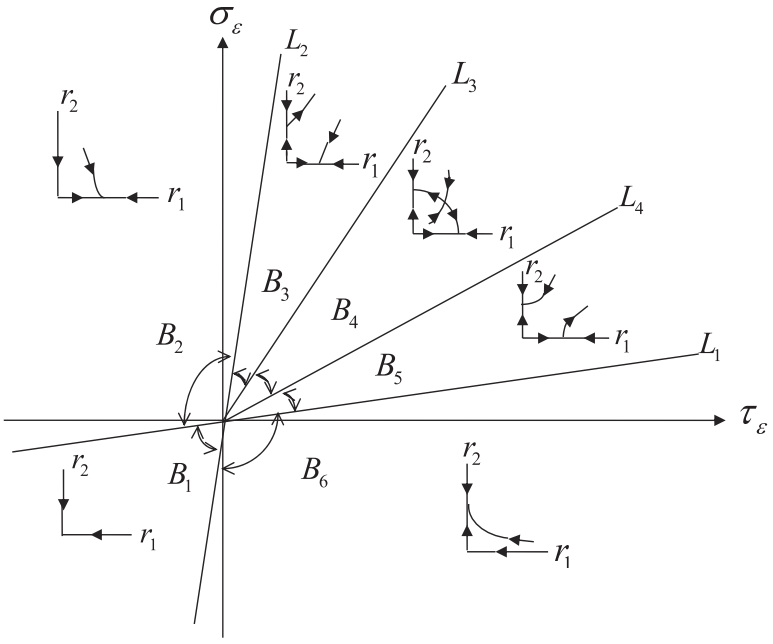

Fig. 7. Critical bifurcation lines in the $(\tau_\varepsilon, \sigma_\varepsilon)$ parameter plane near the non-resonant double Hopf critical point (τ_c, σ_c) and the corresponding phase portraits in the (r_1, r_2) plane.

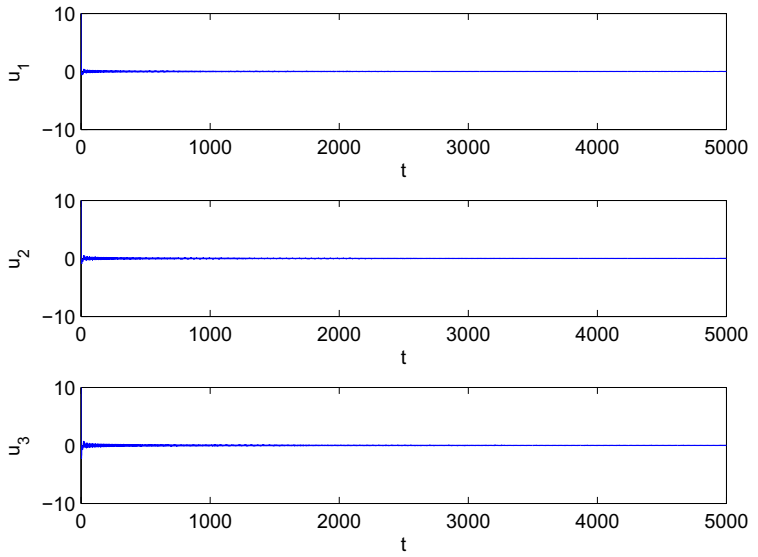

Fig. 8. Simulated solution of system (2) associated with the non-resonant double Hopf bifurcation, for $(\tau_c, \sigma_c) = (13.16190556, 2.028520562)$, $a = -1$, $b = -1.485451766$ and $(\tau_\epsilon, \sigma_\epsilon) = (-0.1, -0.02)$, showing a stable fixed point.

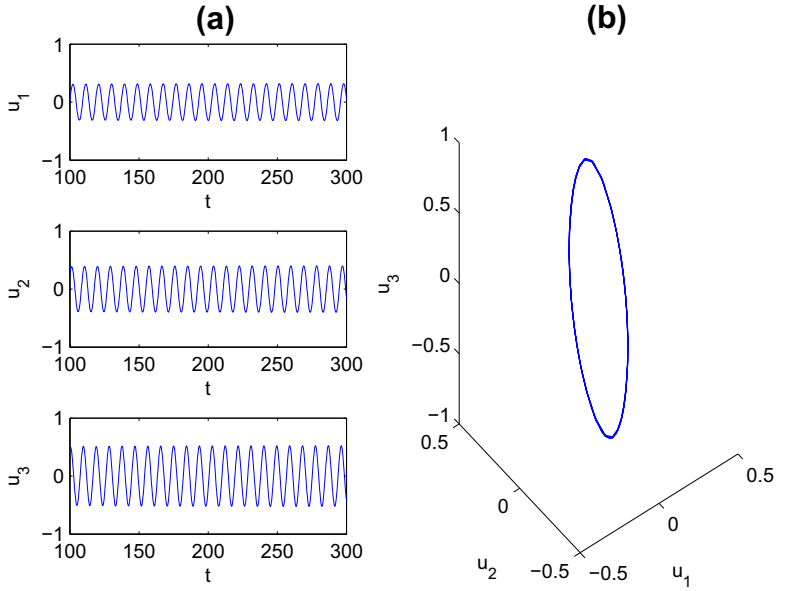

Fig. 9. Simulated solution of system (2) associated with the non-resonant double Hopf bifurcation, for $(\tau_c, \sigma_c) = (13.16190556, 2.028520562)$, $a = -1$, $b = -1.485451766$ and $(\tau_\epsilon, \sigma_\epsilon) = (-0.1, 0.1)$: (a) the time history; and (b) the phase portrait, showing a stable periodic solution.

The semi-trivial equilibrium $\widetilde{F}_1$ bifurcates from the origin on the critical line $L_1 : \mathrm{Re}(\xi_1) = 0$, and its stability is determined by L_1 and $L_3 : \mathrm{Re}(\xi_5) - \frac{\mathrm{Re}(\xi_1)\mathrm{Re}(\xi_7)}{\mathrm{Re}(\xi_2)} = 0$. Anther semi-trivial equilibrium $\widetilde{F}_2$ bifurcates from the origin on the critical line $L_2 : \mathrm{Re}(\xi_5) = 0$, and its stability is determined by L_2 and $L_4 : \mathrm{Re}(\xi_1) - \frac{\mathrm{Re}(\xi_3)\mathrm{Re}(\xi_5)}{\mathrm{Re}(\xi_6)} = 0$. With the general normal form of the resonant double Hopf bifurcation, it is difficult to obtain an explicit expression for the non-trivial equilibria, since it needs to solve coupled equations involving trigonometrical functions. However, we may show analytical results for certain parameter values. For this purpose, we choose $a = -3$ and $b = -1.95251514$. Then all roots of Eq. (4) with $\tau = 0$ have negative real part, and Eq. (6) has only one positive root, $y_1 = 0.04171216744$, and thus, $\upsilon_1 = \sqrt{y_1} = 0.2042355685$. It then follows from (7) that $\tau_1^{(0)} = 13.71312954$. As a result, by Lemma 2.1, all roots of Eq. (4) have negative real part for all $\tau \in [0, \tau_1^{(0)})$. Let

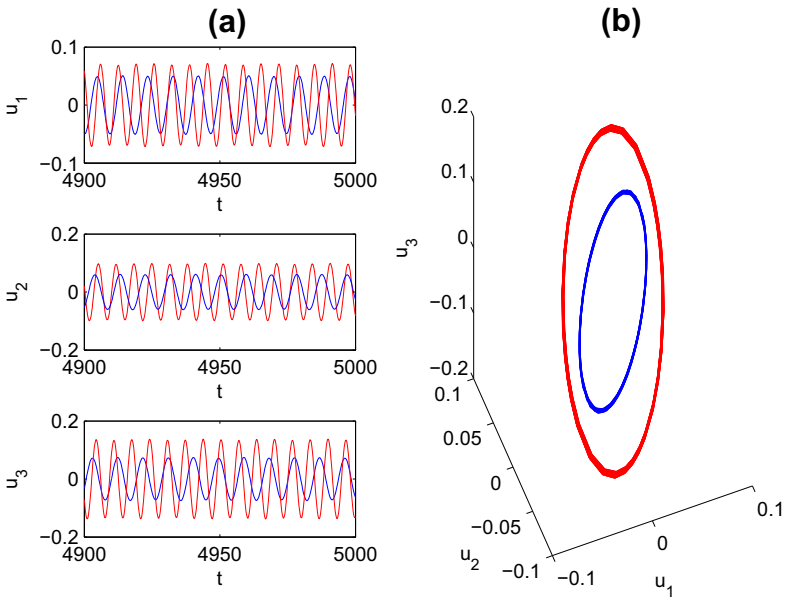

Fig. 10. Simulated solution of system (2) associated with the non-resonant double Hopf bifurcation, for $(\tau_c, \sigma_c) = (13.16190556, 2.028520562)$, $a = -1,\ b = -1.485451766$ and $(\tau_\epsilon, \sigma_\epsilon) = (0.1, 0.021)$: (a) the time history; and (b) the phase portrait, showing coexistence of a pair of stable periodic solutions with the initial values $(x_1(0), x_2(0), x_3(0)) = (1, 1, 1)$ (blue lines) and $(x_1(0), x_2(0), x_3(0)) = (-0.01, -0.01, 0.001)$ (red lines), respectively. (For interpretation of the references to colour in this figure legend, the reader is referred to the web version of this article.)

$\omega_1 : \omega_2 = \frac{k_1}{k_2} = \frac{1}{3}$. Then, choose $\tau = 8.09472152 < \tau_1^{(0)}$, yielding the positive roots $\tilde{\omega}_k$ of (10), the time delay $\sigma_k^{(0)}$ $(k = 1, 2, \ldots, 6)$, and the transversality conditions as follows:

$$
\begin{aligned}
&\tilde{\omega}_1 = 0.2517478606, \quad \sigma_1^{(0)} = 20.77861020, \mathrm{Re}(\lambda'(\sigma_1^{(0)})) < 0,\\
&\tilde{\omega}_2 = 0.3319447390, \quad \sigma_2^{(0)} = 0.4385619315, \mathrm{Re}(\lambda'(\sigma_2^{(0)})) > 0,\\
&\tilde{\omega}_3 = 0.7959334010, \quad \sigma_3^{(0)} = 4.039347823, \mathrm{Re}(\lambda'(\sigma_3^{(0)})) < 0,\\
&\tilde{\omega}_4 = 0.9958342170, \quad \sigma_4^{(0)} = 0.4385619315, \mathrm{Re}(\lambda'(\sigma_4^{(0)})) > 0,\\
&\tilde{\omega}_5 = 1.519160551, \quad \sigma_5^{(0)} = 1.011344435, \mathrm{Re}(\lambda'(\sigma_5^{(0)})) < 0,\\
&\tilde{\omega}_6 = 1.586291511, \quad \sigma_6^{(0)} = 0.6278779457, \mathrm{Re}(\lambda'(\sigma_6^{(0)})) > 0.
\end{aligned}
$$

Therefore, when $a = -3,\ b = -1.95251514,\ \tau = 8.09472152$ and $\sigma = 0.4385619315$, the characteristic Eq. (3) has two pairs of purely imaginary eigenvalues $\pm i\omega_1 = \pm i\tilde{\omega}_2 = \pm 0.3319447390i$ and $\pm i\omega_2 = \pm i\tilde{\omega}_4 = \pm 0.9958342170i$ with $\omega_1 : \omega_2 = \frac{1}{3}$, and all the other eigenvalues have negative real part. Thus, system (2) undergoes a $1:3$ resonant double Hopf bifurcation. With the above parameter values, by using Eq. (36), we obtain the following normal form in polar coordinates:

$$
\begin{aligned}
\frac{dR_1}{dt} &= (0.00029394682\tau_\epsilon + 0.006466566609\sigma_\epsilon)R_1 - 0.1902499902R_1^3 - 0.6405817788R_1R_2^2\\
&\quad - 0.2542333541R_1^2R_2\cos(\Phi) - 0.03567061761R_1^2R_2\sin(\Phi),\\
\frac{dR_2}{dt} &= (0.08088650963\sigma_\epsilon - 0.00116917048\tau_\epsilon)R_2 - 0.4267701161R_2^3 - 0.4608759664R_1^2R_2\\
&\quad - 0.05051277383R_1^3\cos(\Phi) + 0.04555313617R_1^3\sin(\Phi),\\
\frac{d\Theta_1}{dt} &= 0.02324633795\sigma_\epsilon - 0.03518462362\tau_\epsilon - 0.04859791763R_1^2 - 0.2444771570R_2^2\\
&\quad - 0.03567061761R_1R_2\cos(\Phi) + 0.2542333541R_1R_2\sin(\Phi),\\
R_2\frac{d\Theta_2}{dt} &= 0.04873046339\sigma_\epsilon R_2 - 0.1028027384\tau_\epsilon R_2 - 0.4758085568R_2^3 - 0.3727224674R_1^2R_2\\
&\quad - 0.04555313617R_1^3\cos(\Phi) - 0.05051277383R_1^3\sin(\Phi),
\end{aligned}
\tag{39}
$$

where $\Phi = 3\Theta_1 - \Theta_2$. Note that in this case, the non-trivial steady-state solutions are obtained by solving the three equations: $\dot{R}_1 = \dot{R}_2 = 0$ and $\dot{\Phi} = 3\dot{\Theta}_1 - \dot{\Theta}_2 = 0$. The stability of the steady-state solutions is determined by the eigenvalues of the following Jacobin matrix:

$$J=\begin{pmatrix} \frac{\partial \dot{R}_1}{\partial R_1} & \frac{\partial \dot{R}_1}{\partial R_2} & \frac{\partial \dot{R}_1}{\partial \Phi} \\ \frac{\partial \dot{R}_2}{\partial R_1} & \frac{\partial \dot{R}_2}{\partial R_2} & \frac{\partial \dot{R}_2}{\partial \Phi} \\ \frac{\partial \dot{\Phi}_1}{\partial R_1} & \frac{\partial \dot{\Phi}_1}{\partial R_2} & \frac{\partial \dot{\Phi}_1}{\partial \Phi} \end{pmatrix}.$$

Under the given parameter values, we obtain

$$L_1:\sigma_\epsilon=-0.04545639715\tau_\epsilon,\quad L_2:\sigma_\epsilon=0.01445445582\tau_\epsilon,$$
$$L_3:\sigma_\epsilon=0.02884404818\tau_\epsilon,\quad L_4:\sigma_\epsilon=0.01782494356\tau_\epsilon.$$

Next, we consider the existence and stability of non-trivial equilibria of (39). First, we solve the two equations, $\dot{R}_1=\dot{R}_2=0$, to obtain $\cos(\Phi)$ and $\sin(\Phi)$ expressed in $R_1,\ R_2,\ \tau_\epsilon$ and σ_ϵ. Substituting these expressions into the equation $\dot{\Phi}=3\dot{\Theta}_1-\dot{\Theta}_2=0$, and using the identity $\cos^2(\Phi)+\sin^2(\Phi)=1$, we get two equations expressed only in $R_1,\ R_2,\ \tau_\epsilon$ and σ_ϵ. From these two equations, we obtain the first-order approximate solution of R_1 and R_2, expressed in τ_ϵ and σ_ϵ. Note that the first-order approximate solution is sufficient for local dynamical analysis. Therefore, the existence of non-trivial equilibrium solutions can be determined by $R_1>0$ and $R_2>0$, namely, $(\tau_\epsilon,\sigma_\epsilon)\in\{(\tau_\epsilon,\sigma_\epsilon):\sigma_\epsilon>L_1,\sigma_\epsilon>L_5\}$, where $L_5:\sigma_\epsilon=-0.03796464187\tau_\epsilon$. Next, substituting the expressions of $\cos(\Phi),\ \sin(\Phi),\ R_1$ and R_2 into the characteristic equation $\det(\lambda \mathrm{I}-J)=0$, results in a polynomial equation, $\lambda^3+a_2(\tau_\epsilon,\sigma_\epsilon)\lambda^2+a_1(\tau_\epsilon,\sigma_\epsilon)\lambda+a_0(\tau_\epsilon,\sigma_\epsilon)=0$. Hence, the equilibrium solution is stable if $a_2>0,\ a_0>0$ and $a_1a_2-a_0>0$, namely, $(\tau_\epsilon,\sigma_\epsilon)\in\{(\tau_\epsilon,\sigma_\epsilon):\sigma_\epsilon<L_3,\sigma_\epsilon>L_6\}$, where $L_6:\sigma_\epsilon=-0.03450897548\tau_\epsilon$.

Fig. 11 shows the critical bifurcation lines in the $(\tau_\epsilon,\sigma_\epsilon)$ parameter plane near the critical point (τ_c,σ_c) and the corresponding phase portraits in the (R_1,R_2) plane, with the origin representing the resonant double Hopf bifurcation critical point.

For system (2), we use Fig. 11 to describe the bifurcations near the resonant double Hopf bifurcation critical point in the clockwise direction, starting from $\widetilde{B}_1$ and ending at $\widetilde{B}_1$. First, in region $\widetilde{B}_1$, there is only one trivial equilibrium which is a sink. When the parameters are varied across the line L_2 from region $\widetilde{B}_1$ to $\widetilde{B}_2$, the trivial equilibrium becomes a saddle, and a stable semi-trivial solution $\widetilde{O}_2$ appears from the trivial solution. When the parameters are changed from region $\widetilde{B}_2$ to $\widetilde{B}_3$, an unstable semi-trivial solution $\widetilde{O}_1$ occurs from the trivial solution, while a periodic-three solution $\widetilde{O}_3$ appears, which is a saddle, and the trivial fixed point becomes a source from a saddle. In region $\widetilde{B}_4$, $\widetilde{O}_1$ becomes a sink from a saddle, while $\widetilde{O}_3$ becomes a sink from a saddle. When the parameters are further changed from region $\widetilde{B}_4$ to $\widetilde{B}_5$ crossing the line $L_4,\ \widetilde{O}_3$ becomes a stable focus from a sink. When the parameters are further varied across the line L_2 from region $\widetilde{B}_5$ to

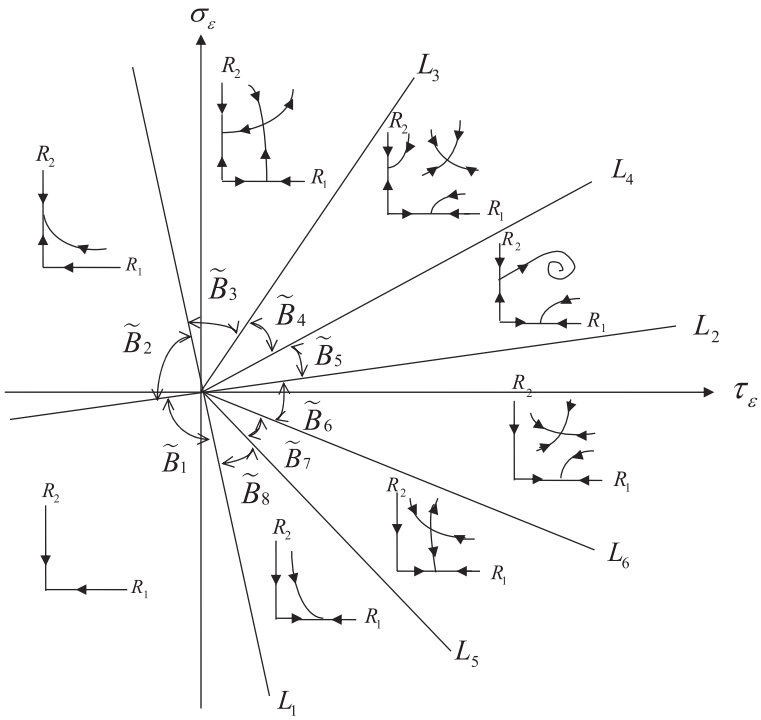

Fig. 11. Critical bifurcation lines in the $(\tau_\epsilon,\sigma_\epsilon)$ parameter plane near the 1:3 resonant double Hopf critical point (τ_c,σ_c) and the corresponding phase portraits in the (R_1,R_2) plane.

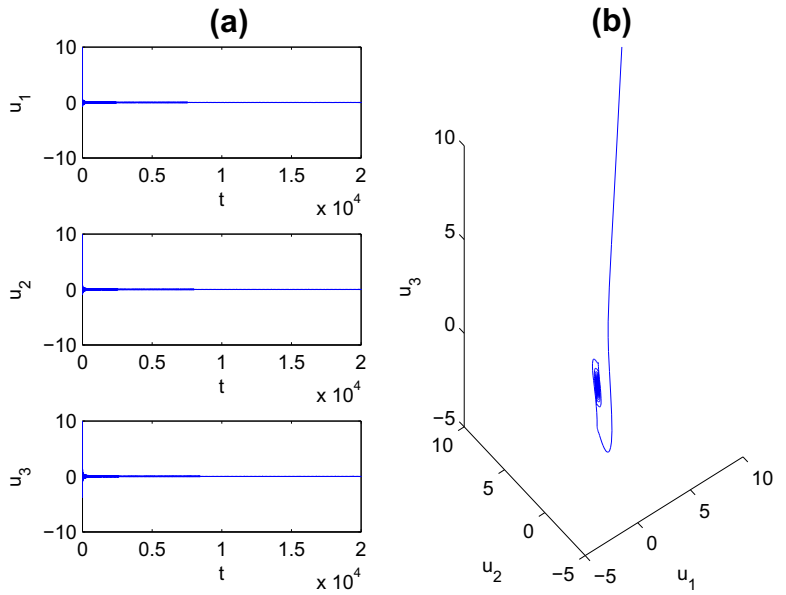

Fig. 12. Simulated solution of system (2) associated with the 1:3 resonant double Hopf bifurcation for $(\tau_c, \sigma_c) = (8.09472152, 0.4385619315)$, $a = -3$, $b = -1.95251514$ and $(\tau_\epsilon, \sigma_\epsilon) = (-0.1, -0.02)$: (a) the time history; and (b) the phase portrait, showing a stable fixed point.

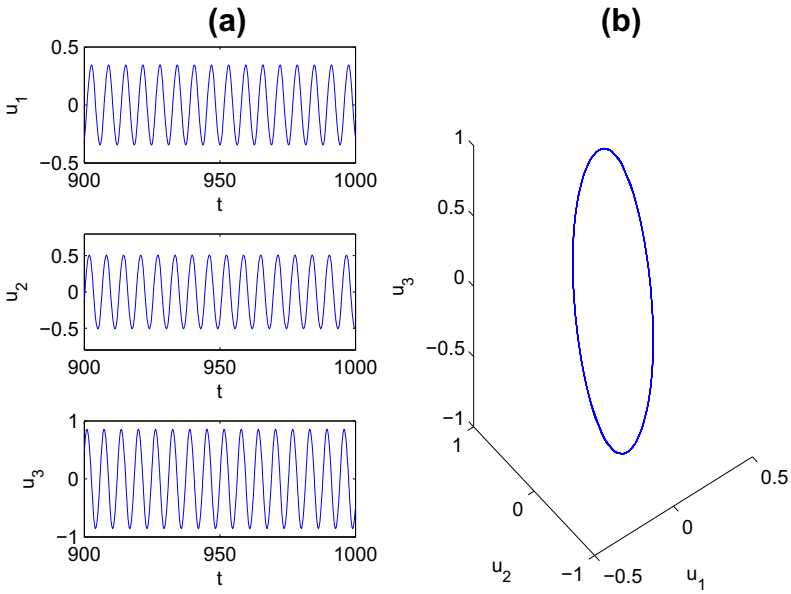

Fig. 13. Simulating solution of system (2) associated with the 1:3 resonant double Hopf bifurcation for $(\tau_c, \sigma_c) = (8.09472152, 0.4385619315)$, $a = -3$, $b = -1.95251514$ and $(\tau_\epsilon, \sigma_\epsilon) = (-0.1, -0.02)$: (a) the time history; and (b) the phase portrait, showing a stable periodic solution.

$\widetilde{B}_6$, $\widetilde{O}_2$ collides with the trivial solution and then disappears, while the trivial solution becomes a saddle from a source, and $\widetilde{O}_3$ becomes a sink from a focus. In region $\widetilde{B}_7$, $\widetilde{O}_3$ becomes a saddle from a sink. In region $\widetilde{B}_8$, $\widetilde{O}_3$ collides with the semi-trivial solution $\widetilde{O}_1$ and then disappears. Finally, when the parameters are varied across the line L_1 from region $\widetilde{B}_8$ to $\widetilde{B}_1$, the stable periodic solution $\widetilde{O}_1$ collides with the trivial solution and then disappears, and the trivial solution becomes a sink from a saddle.

For numerical simulation, we choose three groups of perturbation parameter values: $(\tau_\epsilon, \sigma_\epsilon) = (-0.01, -0.01)$, $(-0.1, 0.2)$, and $(0.1, 0.0003)$, which belong to the regions $\widetilde{B}_1$, $\widetilde{B}_2$ and $\widetilde{B}_6$, corresponding to a stable fixed point shown in Fig. 12, a stable periodic solution as depicted in Fig. 13, and coexistence of a pair of stable periodic solutions shown in Fig. 14, respectively.

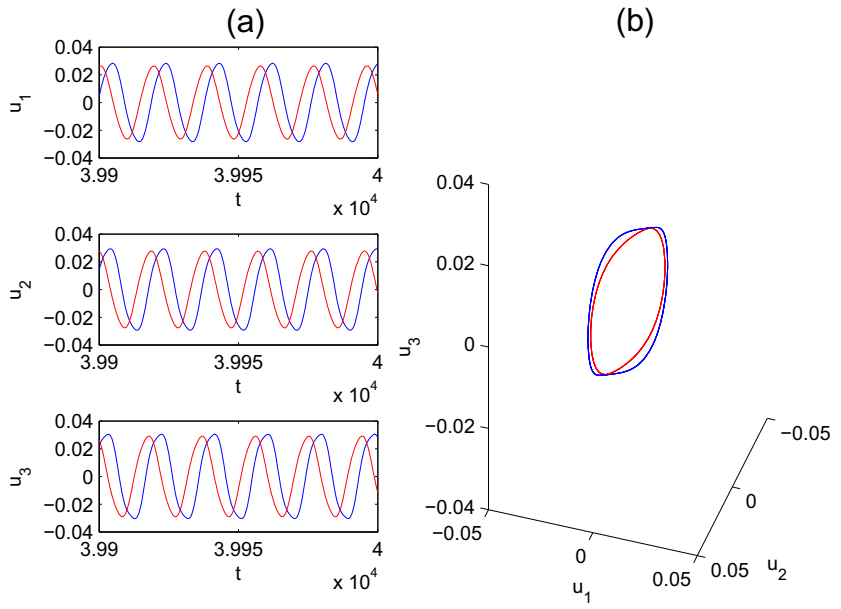

Fig. 14. Simulating solution of (2) associated with the 1:3 resonant double Hopf bifurcation for $(\tau_c,\sigma_c)=(8.09472152,0.4385619315)$, $a=-3,\ b=-1.95251514$ and $(\tau_\epsilon,\sigma_\epsilon)=(-0.1,-0.02)$: (a) the time history; and (b) the phase portrait, showing coexistence of a pair of stable periodic solutions with the initial values $(x_1(0),x_2(0),x_3(0))=(1,1,1)$ (blue lines) and $(x_1(0),x_2(0),x_3(0))=(-0.01,-0.01,0.01)$ (red lines), respectively. (For interpretation of the references to colour in this figure legend, the reader is referred to the web version of this article.)

For $(\tau_\epsilon,\sigma_\epsilon)=(-0.1,0.2)\in\widetilde{B}_2$, $\widetilde{F}_2=(0,R_2)=\left(0,\sqrt{-\frac{\mathrm{Re}(\xi_5)}{\mathrm{Re}(\xi_6)}}\right)=(0,0.1953978468)$, note that $\omega_2=3\omega_0=0.995834217$, and so the period of the periodic solution $\widetilde{O}_2$ is $\frac{2\pi}{\omega_2}\approx 6.3$, implying that there are about $\frac{100}{6.3}\approx 15.85$ periods in 100 time unit, which agrees well with the numerical simulation result (see Fig. 13).

Substituting $K_1=0$ and $K_2=R_2e^{i\Theta_2}$ into (31) yields the first-order approximation of the periodic solution $\widetilde{O}_2$, given below:

$$u^{(1)}=R_2q_2e^{3i\omega_0T_0+i\theta_2}+R_2\bar{q}_2e^{-3i\omega_0T_0-i\theta_2}=2R_2\begin{pmatrix}\cos(3\omega_0T_0+\theta_2)\\ \cos(3\omega_0T_0+\theta_2)-3\omega_0\sin(3\omega_0T_0+\theta_2)\\ (1-9\omega_0^2)\cos(3\omega_0T_0+\theta_2)-6\omega_0\sin(3\omega_0T_0+\theta_2)\end{pmatrix}$$
$$\approx\begin{pmatrix}0.3908\cos(3\omega_0T_0+\theta_2)\\ 0.5515\cos(3\omega_0T_0+\theta_2-v_1)\\ 0.7783\cos(3\omega_0T_0+\theta_2-v_2)\end{pmatrix},$$

where v_1 and v_2 are determined by $\tan(v_1)=-3\omega_0$ and $\tan(v_2)=\frac{6\omega_0}{9\omega_0^2-1}$. This indicates that both amplitude and frequency of the motion obtained from the analytical solutions agree well with the numerical results (see Fig. 13).

For $(\tau_\epsilon,\sigma_\epsilon)=(0.1,0.0003)\in\widetilde{B}_6$, $\widetilde{F}_1=(R_1,0)=\left(\sqrt{-\frac{\mathrm{Re}(\xi_1)}{\mathrm{Re}(\xi_2)}},0\right)=(0.01283364773,0)$. Due to $\omega_1=\omega_0=0.3319442739$, the period of the periodic solution $\widetilde{O}_1$ is $\frac{2\pi}{\omega_1}\approx 18.9$, indicating that there are about $\frac{100}{18.9}\approx 5.28$ periods in 100 time unit, which agrees well with the numerical simulation result (see the blue lines in Fig. 14).

Substituting $K_1=R_1e^{i\Theta_1}$ and $K_2=0$ into (31) yields the first-order approximate solution of the periodic solution $\widetilde{O}_1$ as follows:

$$u^{(1)}=R_1q_1e^{i\omega_0T_0+i\theta_1}+R_1\bar{q}_1e^{-i\omega_0T_0-i\theta_1}=2R_1\begin{pmatrix}\cos(\omega_0T_0+\theta_1)\\ \cos(\omega_0T_0+\theta_1)-\omega_0\sin(\omega_0T_0+\theta_1)\\ (1-\omega_0^2)\cos(\omega_0T_0+\theta_)-2\omega_0\sin(\omega_0T_0+\theta_1)\end{pmatrix}$$
$$\approx\begin{pmatrix}0.0257\cos(\omega_0T_0+\theta_1)\\ 0.0270\cos(\omega_0T_0+\theta_1-v_3)\\ 0.0285\cos(\omega_0T_0+\theta_1-v_4)\end{pmatrix},$$

where v_3 and v_4 are determined by $\tan(v_3)=-\omega_0$ and $\tan(v_4)=\frac{2\omega_0}{\omega_0^2-1}$. This again shows that the analytical prediction of both amplitude and frequency of the motion agree well with the numerical results (see the blue lines in Fig. 14).

Non-trivial equilibrium solutions can be solved from the three equations, $\dot{R}_1=\dot{R}_2=\dot{\Phi}=0$ numerically, to obtain an approximate solution. For $(\tau_\epsilon,\sigma_\epsilon)=(0.1,0.0003)\in\widetilde{B}_6$, we obtain $R_1=0.1272239961$, $R_2=0.0004960617624$ and

$\Phi = 1.471379268$, and the eigenvalues of the Jacobian matrix J evaluated at this non-trivial equilibrium all have negative real part, clearly indicating that this resonant steady-state periodic solution is asymptotically stable.

Substituting $K_1 = R_1 e^{i\theta_1}$ and $K_2 = R_2 e^{i\theta_2}$ into (31), we obtain the first-order approximate solution of system (2) as follows:

$$\begin{aligned} u^{(1)} &= R_1 q_1 e^{i\omega_0 T_0 + i\theta_1} + R_1 \bar{q}_1 e^{-i\omega_0 T_0 - i\theta_1} + R_2 q_2 e^{3i\omega_0 T_0 + i\theta_2} + R_2 \bar{q}_2 e^{-3i\omega_0 T_0 - i\theta_2} \\ &= 2R_1 \begin{pmatrix} \cos(\omega_0 T_0 + \theta_1) \\ \cos(\omega_0 T_0 + \theta_1) - \omega_0 \sin(\omega_0 T_0 + \theta_1) \\ (1-\omega_0^2)\cos(\omega_0 T_0 + \theta_1) - 2\omega_0 \sin(\omega_0 T_0 + \theta_1) \end{pmatrix} \\ &\quad + 2R_2 \begin{pmatrix} \cos(3\omega_0 T_0 + \theta_2) \\ \cos(3\omega_0 T_0 + \theta_2) - 3\omega_0 \sin(3\omega_0 T_0 + \theta_2) \\ (1-9\omega_0^2)\cos(3\omega_0 T_0 + \theta_2) - 6\omega_0 \sin(3\omega_0 T_0 + \theta_2) \end{pmatrix} \\ &\approx \begin{pmatrix} 0.2544\cos(\omega_0 T_0 + \theta_1) + 9.9212 \times 10^{-4}\cos(3\omega_0 T_0 + \theta_2) \\ 0.2681\cos(\omega_0 T_0 + \theta_1 - v_3) + 1.4002 \times 10^{-3}\cos(3\omega_0 T_0 + \theta_2 - v_1) \\ 0.2825\cos(\omega_0 T_0 + \theta_1 - v_4) + 1.9760 \times 10^{-3}\cos(3\omega_0 T_0 + \theta_2 - v_2) \end{pmatrix}, \end{aligned}$$

where $v_j's$ $(j = 1,2,3,4)$ are determined by $\tan(v_1) = -3\omega_0$ and $\tan(v_2) = \frac{6\omega_0}{9\omega_0^2 - 1}$, $\tan(v_3) = -\omega_0$ and $\tan(v_4) = \frac{2\omega_0}{\omega_0^2 - 1}$. Comparing these analytical predictions with the numerical simulation results (see the red lines in Fig. 14), it shows an excellent agreement.

6. Conclusion

In this paper, we have studied the dynamical behaviors of a three-node recurrent neural network model with four discrete time delays. We have analysed the stability of the trivial equilibrium and the existence of several types of bifurcation. To study dynamical motion, we have used the multiple time scales method to derive the normal forms associated with Hopf-zero bifurcation, non-resonant and resonant double Hopf bifurcations. Moreover, bifurcation analyses near the Hopf-zero, non-resonant and resonant double Hopf critical points are given, showing that system (2) may, associated with Hopf-zero bifurcation, exhibit a stable fixed point, a pair of stable fixed points, a stable periodic solution, and coexistence of a pair of stable fixed points and a stable periodic solution; and, associated with non-resonant double Hopf bifurcation, a stable fixed point, a stable periodic solution and coexistence of a pair of stable periodic solutions. Numerical simulations are presented to verify the analytical predictions. In particular, for the resonant double Hopf bifurcation, although closed-form solution of the non-trivial steady-state solutions is difficult to obtain, we obtain numerical expressions for certain parameter values. The excellent agreement of the solutions of amplitude and frequency between the analytical predictions and numerical simulations shows that the method presented in this paper may provide a very good tool in the study of real problems.

Acknowledgments

This work was supported by the National Natural Science Foundation of China (NSFC) and the National Science and Engineering Research Council of Canada (NSERC), the Heilongjiang Provincial Natural Science Foundation (No. A200806), and the Program of Excellent Team in HIT. The first author also acknowledges the financial support received from the China Scholarship Council for her visiting the University of Western Ontario.

References

[1] Campbell SA, Yuan Y, Bungay SD. Equivariant Hopf bifurcation in a ring of identical cells with delayed coupling. Nonlinearity 2005;18:2827–46.
[2] Choi Y, LeBlanc VG. Toroidal normal forms for bifurcations in retarded functional differential equations I: multiple Hopf and transcritical/multiple Hopf interaction. J Differ Equat 2006;227:166–203.
[3] Das SL, Chatterjee A. Multiple scales without center manifold reductions for delay differential equations near Hopf bifurcations. Nonlinear Dynam 2002;30:323–35.
[4] Ensari T, Arik S. Global stability analysis of neural networks with multiple time varying delays. IEEE Trans Autom Control 2005;50(11):1781–5.
[5] Ensari T, Arik S. Global stability of class of neural networks with time-varying delay. IEEE Trans Circ Syst II. Exp Briefs 2005;52(3):126–30.
[6] Feng C, O'Reilly C, Plamondon R. Permanent oscillations in a 3-node recurrent neural network model. Neurocomputing 2010;74:274–83.
[7] Feng C, Plamondon R, O'Reilly C. On some necessary and sufficient conditions for a recurrent neural network model with time delays to generate oscillations. IEEE Trans Neural Networks 2010;21(8):1197–205.
[8] Feng C, Plamondon R, O'Reilly C. Analyzing oscillations for an N-node recurrent neural networks model with time delays and general activation functions. IEEE Trans Circ Syst I. Regul Pap 2011;58(8):1877–87.
[9] Gao B, Zhang W. Equilibria and their bifurcations in a recurrent neural network involving iterates of a transcendental function. IEEE Trans Neural Networks 2008;19(5):782–94.
[10] Giles CL, Lawrence S, Tsoi AC. Noisy time series prediction using recurrent neural networks and grammatical inference. Mach Learn 2001;44:161–83.
[11] Guo S, Chen Y, Wu J. Two-parameter bifurcations in a network of two neurons with multiple delays. J Differ Equat 2008;244:444–86.
[12] Hajihosseini A, Rokni Lamooki GR, Beheshti B, Maleki F. The Hopf bifurcation analysis on a time-delayed recurrent neural network in the frequency domain. Neurocomputing 2010;73:991–1005.
[13] Hale J. Theory of functional differential equations. New York: Springer-Verlag; 1997.
[14] Harter D, Kozma R. Chaotic neurodynamics for autonomous agents. IEEE Trans Neural Networks 2005;16(3):565–79.

[15] Hu X, Zhang B. An alternative recurrent neural network for solving variational inequalities and related optimization problems. IEEE Trans Syst Man Cybernet B: Cybernet 2009;39(6):1640–5.
[16] Jiang W, Yuan Y. Bogdanov–Takens singularity in van der Pol's oscillator with delayed feedback. Physica D 2007;227(2):149–61.
[17] Maier HR, Dandy GC. Neural networks for the prediction and forecasting of water resources variables: a review of modelling issues and applications. Environ Model Softw 2000;15(1):101–24.
[18] Maleki F, Beheshti B, Hajihosseini A, Rokni Lamooki GR. The Bogdanov–Takens bifurcation analysis on a three dimensional recurrent neural network. Neurocomputing 2010;73:3066–78.
[19] Nayfeh AH. Introduction to perturbation techniques. New York: Wiley-Interscience; 1981.
[20] Nayfeh AH. Order reduction of retarded nonlinear systems–the method of multiple scales versus center-manifold reduction. Nonlinear Dynam 2008;51:483–500.
[21] Park JH. A new stability analysis of delayed cellular neural networks. Appl Math Comput 2006;181(1):200–5.
[22] Parlos AG, Menon SK, Atiya AF. An algorithmic approach to adaptive state filtering using recurrent neural networks. IEEE Trans Neural Networks 2001;12(6):1411–32.
[23] Ruiz A, Owens DH, Townley S. Existence, learning, and replication of periodic motions in recurrent neural networks. IEEE Trans Neural Networks 1998;9(4):651–61.
[24] Song Y. Spatio-temporal patterns of Hopf bifurcating periodic oscillations in a pair of identical tri-neuron network loops. Commun Nonlinear Sci Numer Simul 2012;17(2):943–52.
[25] Townley S, Ilchmann A, Weiss MG, Mcclements W, Ruiz AC, Owens DH, et al. Existence and learning of oscillations in recurrent neural networks. IEEE Trans Neural Networks 2000;11(1):205–14.
[26] Wang B, Jian J. Stability and Hopf bifurcation analysis on a four-neuron BAM neural network with distributed delays. Commun Nonlinear Sci Numer Simul 2010;15(2):189–204.
[27] Wang H, Jiang W. Hopf-pitchfork bifurcation in van der Pol's oscillator with nonlinear delayed feedback. J Math Anal Appl 2010;368(1):9–18.
[28] Wei J, Li MY. Global existence of periodic solutions in a tri-neuron network model with delays. Physica D 2004;198:106–19.
[29] Wei J, Yuan Y. Synchronized Hopf bifurcation analysis in a neural network model with delays. J Math Anal Appl 2005;312(1):205–29.
[30] Yu P. Symbolic computation of normal forms for resonant double Hopf bifurcations using a perturbation technique. J Sound Vib 2001;247(4):615–32.
[31] Yu P. Analysis on double Hopf bifurcation using computer algebra with the aid of multiple scales. Nonlinear Dynam 2002;27:19–53.
[32] Yu W, Cao J. Stability and Hopf bifurcation on a two-neuron system with time delay in the frequency domain. Int J Bifur Chaos 2007;17(4):1355–66.